

Output Feedback MPC with Adaptive Tubes

Anchita Dey*, Graduate Student Member, IEEE, and Shubhendu Bhasin

Abstract—An output feedback model predictive control (MPC) framework with *adaptive tubes* is proposed for linear time-invariant systems subject to parametric and additive uncertainties. An adaptive observer provides point estimates of the system state, model parameters, and initial condition, while jointly updating the corresponding sets containing the true parameters and initial state. These estimates parameterize the constrained optimal control problem, enabling constraint tightening, terminal ingredients, and tube geometry to be updated as the estimates evolve. In contrast to standard robust tube-based MPC formulations, the proposed approach does not require a common quadratically stabilizing linear feedback gain across the parametric uncertainty set. As the available uncertainty information improves, the tube geometry evolves accordingly, resulting in an adaptive tube MPC framework with improved performance over time. Recursive feasibility and robust exponential stability are established, and a numerical example is presented.

Index Terms—Model predictive control (MPC), Uncertain systems, Output feedback and Observers, Constrained control

I. INTRODUCTION

Model predictive control (MPC) is a well-known technique for optimal control of systems subject to hard constraints on states and inputs. Classical MPC [1], [2] relies on a system model to predict future trajectories and compute an optimal control sequence over a finite horizon. The resulting constrained optimal control problem (COCP) requires accurate model knowledge to ensure feasibility and stability. In practice, however, model uncertainty and incomplete state measurements limit the direct applicability of such formulations. Both limitations must be addressed simultaneously in any practically deployable MPC framework.

Robust MPC methods are predominantly formulated either as min-max optimization or LMI-based schemes, or within the robust tube-based framework. These approaches are typically designed for systems with known parameters subject to additive disturbances [3]–[5], or for systems with parametric uncertainty, with or without additive disturbances [6]–[8]. In the latter case, however, no attempt is made to estimate or learn the uncertain parameters. To mitigate conservatism and enhance performance, adaptive MPC has gained attention

[9]–[15]. In these formulations, uncertain parameters, or the sets containing them, or both, are updated online, while robustness to estimation errors is maintained through tube-based constructions. Homothetic tube parameterizations [4], [5] are particularly attractive due to their tractability. Recent works have also explored refined tube representations; [16] proposes flexible tubes based on zonotopes, where the tube cross-sectional parameters are optimized online. The framework in [17] considers systems with additive disturbances and constructs tubes via online blending of precomputed sets associated with different stabilizing feedback gains. Self-tuning tube schemes for systems with both parametric and additive uncertainties are developed in [18]. The recent work in [19] refines classical rigid tube MPC [4] for LTI systems with additive disturbances by introducing time-varying tube cross-sections within a state feedback design framework, while assuming known system parameters.

The MPC frameworks for systems with parametric uncertainty and state constraints, such as [8]–[16], [18], typically assume the existence of a quadratically stabilizing linear state feedback gain valid over the entire uncertainty set [20]. While this assumption enables tractable design, it restricts the admissible uncertainty sets [21], [22], and such a common gain may not exist for all parameter realizations [23]. Data-driven approaches [24], [25] avoid this requirement, but rely on offline representations that may be sensitive to changes in system dynamics and typically impose constraints on inputs and outputs rather than all states.

In this paper, an output feedback MPC framework with adaptive tubes is proposed for discrete-time LTI systems subject to parametric and additive uncertainties. Similar to [14], an adaptive observer is employed together with a reformulated COCP, with two key modifications. First, point estimates of the initial condition are obtained in addition to the state and parameter estimates. Second, available data is used to jointly update the uncertainty sets for the parameters and the initial condition using set membership-based identification [26]. Further, the linear regression for parameter adaptation is augmented by combining past and current data, enabling improved convergence [27]–[29]. To formulate the COCP, the system dynamics is expressed using the current estimates, with the resulting mismatch treated as a lumped additive disturbance. Based on this representation, constraint tightening, terminal set computation, and tube design are carried out as in existing robust tube MPC [5], [30]. The COCP components are designed for the current parameter estimate, and therefore require only a stabilizing feedback gain, terminal cost, and terminal set for that estimate, eliminating the need for a common design across all admissible parametric uncertainties.

This paragraph of the first footnote will contain the date on which you submitted your paper for review.

Anchita Dey and Shubhendu Bhasin are with the department of Electrical Engineering, Indian Institute of Technology Delhi, Hauz Khas, New Delhi, Delhi 110016, India. anchitadey.ee.india@gmail.com, sbhasin@ee.iitd.ac.in.

*Corresponding author

As the estimates and uncertainty sets evolve, the tube geometry and the COCP components change accordingly, leading to an *adaptive tube* MPC framework. While contraction of the uncertainty sets preserves recursive feasibility and stability, the central technical challenge is ensuring that the time-varying COCP retains its stability and feasibility properties despite changes in the prediction model induced by point estimate updates. The proposed solution avoids the standard requirement of a common quadratically stabilizing linear feedback gain over the entire uncertainty set. Instead, a compatibility condition is imposed on the successive terminal ingredients that ensures that the Lyapunov function remains non-increasing along the closed-loop trajectories—a condition that is strictly less restrictive than the quadratic stabilization over the entire uncertainty set. Recursive feasibility is maintained using a backup solution from the previous time step. Improved uncertainty characterization results in tighter prediction bounds, and appending the state estimation error sets to the homothetic tube returned by the COCP yields an outer tube containing the true state trajectory.

The contributions are summarized as follows:

- An adaptive observer design that estimates the initial state along with system parameters and state, and jointly updates the associated uncertainty sets using set membership-based identification.
- An MPC formulation in which the COCP components, including constraint tightening, terminal set, and tube geometry, are updated based on the available estimates.
- Recursive feasibility and robust exponential stability guarantees for the proposed adaptive tube MPC framework, without requiring a common quadratically stabilizing linear feedback gain.

Notations: \oplus denotes Minkowski sum defined as $\mathbb{P} \oplus \mathbb{Q} \triangleq \{p+q \mid p \in \mathbb{P}, q \in \mathbb{Q}\}$ and $p \oplus \mathbb{Q} \triangleq \{p+q \mid q \in \mathbb{Q}\}$. \ominus denotes Pontryagin difference defined as $\mathbb{P} \ominus \mathbb{Q} \triangleq \{p \mid p+q \in \mathbb{P} \forall q \in \mathbb{Q}\}$. The multiplication of any matrix V with a set \mathbb{P} is defined as $V\mathbb{P} \triangleq \{Vp \mid p \in \mathbb{P}\}$, where V and p are of conforming dimensions. For any matrix V , $V(:, p : q)$ and $V(r : s, p : q)$ represent the sub-matrices made of all rows and r -th to s -th rows, respectively, with p -th to q -th columns. The convex hull of all elements in \mathbb{P} is denoted by $\text{co}(\mathbb{P})$. The notation $V \succ 0$ ($\succeq 0$) represents that the matrix V is symmetric positive-definite (positive semi-definite). $\|\cdot\|_\infty$ and $\|\cdot\|_2$ represent ∞ and 2-norms, of a vector (or induced ∞ and 2-norms of a matrix), respectively. $\|p\|_V^2 \triangleq p^\top V p$ for a vector p . The identity matrix and zero matrix are denoted by $I_n \in \mathbb{R}^{n \times n}$ and $0_{m \times n} \in \mathbb{R}^{m \times n}$, respectively. $\{\alpha(i)\}_{i=p:q}$ represents the set $\{\alpha(p), \alpha(p+1), \dots, \alpha(q)\}$, where $\alpha(i)$ is a function of i , and $p, q > p$ are integers. \mathbb{I}_p^q represents the set of all integers from p to q . The value of p at time $t+i$ predicted at time t is denoted by $p_{i|t}$. $(\cdot)^*$ denotes the optimal value returned by solving the COCP. Any signal belonging to \mathcal{L}_∞ implies it is bounded. The operation $\text{vec}(\cdot)$ on a matrix $W = [W_1^\top \ W_2^\top \ \dots \ W_p^\top]^\top \in \mathbb{R}^{p \times q}$, where $W_i^\top \in \mathbb{R}^q \forall i \in \mathbb{I}_1^p$ is defined as $\text{vec}(W) \triangleq [W_1 \ W_2 \ \dots \ W_p]^\top \in \mathbb{R}^{pq}$, and $\text{vec}^{-1}(\cdot, \cdot)$ is the inverse operation of $\text{vec}(\cdot)$, i.e., $\text{vec}^{-1}([W_1 \ W_2 \ \dots \ W_p]^\top, q) \triangleq W$.

II. PROBLEM STATEMENT

The objective is to stabilize the origin of a discrete-time LTI system in the following observable canonical realization:

$$x_{t+1} = \underbrace{\begin{bmatrix} \mathcal{A} & I_{n-q} \\ & 0_{q \times (n-q)} \end{bmatrix}}_{=:A} x_t + B u_t + d_t \quad (1a)$$

$$y_t = \underbrace{\begin{bmatrix} I_q & 0_{q \times (n-q)} \end{bmatrix}}_{=:C} x_t \quad (1b)$$

subject to hard constraints

$$x_t \in \mathbb{X}, u_t \in \mathbb{U} \quad \forall t \in \mathbb{I}_0^\infty. \quad (2)$$

Here, $x_t \in \mathbb{R}^n$, $u_t \in \mathbb{R}^m$, $y_t \in \mathbb{R}^q$, and $d_t \in \mathbb{R}^n$ denote the state, input, output, and disturbance at time t , respectively. The disturbance d_t and the parameters $\mathcal{A} \in \mathbb{R}^{n \times q}$, $B \in \mathbb{R}^{n \times m}$ are unknown. Only output measurements y_t are available. The constraint sets \mathbb{X} and \mathbb{U} are known convex polytopes containing their respective origins in the interior.

To ensure robust feasibility and stability, it is standard to assume that uncertainties belong to known bounded sets [1]–[4], [6]–[12], [14], [15], [17]–[19]. For the problem of interest, the additive and parametric uncertainties are assumed to lie in known convex bounded sets, with $d_t \in \mathbb{D} \subseteq \mathbb{R}^n$ and $\psi \triangleq [\hat{A} \ \hat{B}] \in \Psi \subseteq \mathbb{R}^{n \times (n+m)}$. The set \mathbb{D} is a polytope containing the origin in its interior. The set Ψ is defined as

$$\Psi \triangleq \text{co}(\psi^{[1]}, \psi^{[2]}, \dots, \psi^{[L_p]}), \quad (3)$$

where L_p is a known finite positive integer. For each $\hat{\psi} \triangleq [\hat{A} \ \hat{B}] \in \Psi$, there exists a pair (P, K) specific to $\hat{\psi}$ such that $P \succ 0$ and

$$P - (\hat{A} + \hat{B}K)^\top P (\hat{A} + \hat{B}K) - Q - K^\top R K \succeq 0, \quad (4)$$

for given weighting matrices $Q, R \succ 0$, with $P, Q \in \mathbb{R}^{n \times n}$, $R \in \mathbb{R}^{m \times m}$, and $K \in \mathbb{R}^{m \times n}$. This condition ensures that each system corresponding to $\hat{\psi} \in \Psi$ is stabilizable and admits a quadratic Lyapunov function of the form $x^\top P x$ under a suitable linear state feedback gain $K = -(R + B^\top P B)^{-1} B^\top P A$, and is a standard assumption in MPC formulations [1], [4], [5]. Unlike standard robust tube MPC formulations that require a common quadratically stabilizing feedback gain over the entire uncertainty set [8]–[16], [18], condition (4) only assumes existence of a stabilizing pair for each admissible parameter realization individually¹.

Further, a known convex polytope $\mathbb{X}_0 \subseteq \mathbb{X}$ with L_x vertices is considered for the initial state x_0 , where L_x is a known finite positive integer.

In the ideal case, when the states and parameters are known and no disturbance is present, the origin of (1) can be stabilized

¹This distinction is exploited later in the proposed adaptive tube MPC framework.

by implementing the classical MPC COCP given below.

$$\begin{aligned} & \min_{\{u_i|_t\}_{i=0:N-1}} \sum_{i=0}^{N-1} (\|x_{i+1}|_t\|_Q^2 + \|u_i|_t\|_R^2) + \|x_{N|t}\|_P^2 \\ & \text{subject to } x_{0|t} = x_t, \\ & \quad x_{i+1}|_t = Ax_{i|t} + Bu_{i|t} \quad \forall i \in \mathbb{I}_0^{N-1}, \\ & \quad x_{i|t} \in \mathbb{X} \quad \forall i \in \mathbb{I}_0^N, \quad u_{i|t} \in \mathbb{U} \quad \forall i \in \mathbb{I}_0^{N-1}, \\ & \quad x_{N|t} \in \mathbb{X}_{TS} \subseteq \mathbb{X}, \end{aligned}$$

where N is the prediction horizon length, and \mathbb{X}_{TS} is the terminal set [1, Ch. 2]. The set \mathbb{X}_{TS} is generally constructed to be the maximal positive invariant set for the dynamics $z_{t+1} = (A + BK)z_t$ with admissibility to constraints $\mathbb{X}_{TS} \subseteq \mathbb{X}$ and $K\mathbb{X}_{TS} \subseteq \mathbb{U}$.

Due to parameter uncertainty, external disturbance and unavailability of full state information, this COCP cannot be directly implemented. An alternative is to estimate these quantities online and reformulate the COCP to account for estimation errors and disturbances, as explored in [14], [15].

However, these approaches, along with several tube-based MPC formulations for systems with parametric uncertainty [8]–[13], [16], [18], rely on the existence of a quadratically stabilizing linear feedback gain over the uncertainty set. This requirement stems from the use of a single COCP designed to accommodate all admissible uncertainties.

The objective of this work is therefore to develop an output feedback MPC framework for stabilizing the origin of (1), while maintaining recursive feasibility, robust constraint satisfaction of (2), and stability, without requiring a common quadratically stabilizing linear feedback gain over the entire uncertainty set. To this end, an adaptive observer is employed to obtain online point and set estimates of the uncertain parameters and initial condition. These updated uncertainty descriptions are subsequently incorporated into the COCP through the constraint tightening, terminal ingredients, and tube construction. As the uncertainty sets and point estimates evolve with incoming data, the associated tube geometry also changes accordingly, leading to an adaptive tube MPC framework with progressively reduced conservatism. The adaptive observer is designed in the following section.

III. ADAPTIVE OBSERVER WITH SET-MEMBERSHIP IDENTIFICATION

The plant dynamics in (1a) can be rewritten as

$$\begin{aligned} x_{t+1} &= Fx_t + (A - F)x_t + Bu_t + d_t, \\ &= Fx_t + \underbrace{[Y_t \quad U_t] \begin{bmatrix} (a - f)^\top & b^\top \end{bmatrix}}_{=:p} + d_t, \end{aligned} \quad (5)$$

where $p \in \mathbb{R}^{qn+mn}$, $Y_t \triangleq I_n \otimes y_t^\top \in \mathbb{R}^{n \times qn}$, $U_t \triangleq I_n \otimes u_t^\top \in \mathbb{R}^{n \times mn}$, and $F \in \mathbb{R}^{n \times n}$ is a user-defined Schur stable matrix structurally similar to A in (1a) given by,

$$F \triangleq \begin{bmatrix} \mathcal{F} & \\ & I_{n-q} \\ & & 0_{q \times (n-q)} \end{bmatrix}, \quad \text{where } \mathcal{F} \in \mathbb{R}^{n \times q} \quad (6)$$

$$\text{and } a \triangleq \text{vec}(A) \in \mathbb{R}^{qn}, \quad b \triangleq \text{vec}(B) \in \mathbb{R}^{mn}, \quad (7)$$

$$f \triangleq \text{vec}(\mathcal{F}) \in \mathbb{R}^{qn}. \quad (8)$$

The mapping from ψ to p for a given f is a bijection, and therefore, it suffices to estimate p , which belongs to the set

$$\Pi \triangleq \{Z_1(\bar{\psi}, f, q) \mid \forall \bar{\psi} \in \Psi, f \text{ in (8)}\}. \quad (9)$$

The explicit definitions of the bijective mapping Z_1 and its inverse are provided in Appendix I for completeness. The inverse mapping is used later to recover the estimate of ψ (and therefore of A and B) from the estimate of p .

A. Formulation of filter-based regression

To estimate p and x_t using u_t and y_t , filter matrices $M_t \in \mathbb{R}^{n \times (qn+mn)}$ are defined to construct a linear regression. The filter variables are computed using the dynamics

$$M_{t+1} = FM_t + [Y_t \quad U_t], \quad M_0 = 0_{n \times (qn+mn)}. \quad (10)$$

The plant state and output can then be expressed as

$$x_t = M_t p + F^t x_0 + \sum_{k=0}^{t-1} F^{t-1-k} d_k, \quad (11a)$$

$$y_t = CM_t p + CF^t x_0 + \underbrace{C \sum_{k=0}^{t-1} F^{t-1-k} d_k}_{=: \eta_t}, \quad (11b)$$

respectively. Let \hat{p}_t and \hat{x}_{0_t} be the estimates of p and x_0 , respectively, at time t . The adaptive observer state and output are then defined as

$$\hat{x}_t = M_t \hat{p}_t + F^t \hat{x}_{0_t}, \quad (12a)$$

$$\hat{y}_t = CM_t \hat{p}_t + CF^t \hat{x}_{0_t} = \underbrace{[CM_t \quad CF^t]}_{=: \omega_t} \underbrace{\begin{bmatrix} \hat{p}_t \\ \hat{x}_{0_t} \end{bmatrix}}_{=: \hat{\theta}_t}, \quad (12b)$$

respectively, where $\omega_t \in \mathbb{R}^{q \times (qn+mn+n)}$ is the regressor, and $\hat{\theta}_t \in \mathbb{R}^{qn+mn+n}$ is the estimate of

$$\theta \triangleq [p^\top \quad x_0^\top]^\top \in \mathbb{R}^{qn+mn+n}. \quad (13)$$

Since $x_0 \in \mathbb{X}_0$, the choice of the initial state estimate \hat{x}_{0_t} is restricted to \mathbb{X}_0 . Let the set containing the initial state estimation error \tilde{x}_{0_t} be given by

$$\tilde{\mathbb{X}}_{0_t} \triangleq \{x \mid x + \hat{x}_{0_t} \in \mathbb{X}_0\}. \quad (14)$$

Then, $\tilde{\mathbb{X}}_{0_0}$ is a known convex polytope containing the origin. In addition, for characterizing bounded sets for the state estimation errors $\tilde{x}_t \triangleq x_t - \hat{x}_t$, the following standard assumption is made [14], [15], [31]–[33].

Assumption 1: The set $\tilde{\mathbb{X}}_{0_0} \triangleq \mathbb{X}_0 \ominus \hat{x}_{0_0}$ is positive invariant to the dynamics $z_{t+1} = Fz_t$, i.e.,

$$F\tilde{\mathbb{X}}_{0_0} \subseteq \tilde{\mathbb{X}}_{0_0}. \quad (15)$$

Remark 1: If the given set \mathbb{X}_0 does not satisfy (15), a suitable outer approximation can be used to ensure invariance.

B. Modification of the linear regression

While an update law for learning θ can be derived using (12b), the regressors are further modified to improve convergence of the observer by including an additional $qn + mn + n - 1$ independent error signals [27], [28]. Additionally, update laws for the uncertainty sets Ψ and \mathbb{X}_0 are constructed using the modified regression. To this end, define the following matrices:

$$\mathcal{W}_t \triangleq \begin{bmatrix} \omega_{t(0)}^\top & \omega_{t(1)}^\top & \dots & \omega_{t(qn+mn+n-1)}^\top \end{bmatrix}^\top \in \mathbb{R}^{q(qn+mn+n) \times (qn+mn+n)}, \quad (16a)$$

$$\mathcal{Y}_t \triangleq \begin{bmatrix} y_{t(0)}^\top & y_{t(1)}^\top & \dots & y_{t(qn+mn+n-1)}^\top \end{bmatrix}^\top \in \mathbb{R}^{q(qn+mn+n)}, \quad (16b)$$

where the elements $\omega_{t(i)}$ and $y_{t(i)}$ are generated recursively using exponentially weighted filtering of current and past data, such that the following relation (similar to (11b)) holds.

$$y_{t(i)} = \omega_{t(i)} \theta + \eta_{t(i)}, \quad (17)$$

where $\eta_{t(i)} \in \mathcal{N}_{t(i)}$ that are generated recursively from the disturbance bounds. The detailed recursive laws are given in Appendix II.

C. Adaptation law

At each t , the signals \mathcal{Y}_t and \mathcal{W}_t are available, which allows computation of a non-falsified set for the true quantity θ using (17), (49), and consequently, updating of the uncertainty sets Ψ and \mathbb{X}_0 using set membership identification [26]. The non-falsified set is defined as

$$\Xi_t \triangleq \left\{ (\bar{p}, \bar{x}_0) \mid y_{t(i)} - \omega_{t(i)} [\bar{p}^\top \bar{x}_0^\top]^\top \in \mathcal{N}_{t(i)} \forall (\bar{x}_0, \bar{p}, i) \in \mathbb{R}^n \times \mathbb{R}^{qn+mn} \times \mathbb{I}_0^{qn+mn+n-1} \right\}, \quad (18)$$

where $\Xi_t \in \mathbb{R}^{qn+mn} \times \mathbb{R}^n$. The sets Ψ and \mathbb{X}_0 are updated as

$$\Pi_{t+1} \times \mathbb{X}_{0,t+1} \triangleq \{\Pi_t \times \mathbb{X}_{0,t}\} \cap \Xi_{t+1} \quad (19)$$

$$\Psi_{t+1} \triangleq \{\mathcal{Z}_1^{-1}(\bar{p}, f, q) \mid \forall \bar{p} \in \Pi_{t+1}, f \text{ in (8)}\} \quad (20)$$

with the initial sets

$$\Psi_0 \triangleq \Psi, \quad \Pi_0 \triangleq \Pi, \quad \mathbb{X}_{0,0} \triangleq \mathbb{X}_0. \quad (21)$$

The adaptation of the sets $\mathbb{X}_{0,t}$ and Ψ_t may also lead to a change in the number of their vertices, denoted by L_{x_t} and L_{p_t} , respectively, with

$$L_{x_0} \triangleq L_x, \quad L_{p_0} \triangleq L_p. \quad (22)$$

The reduction in the uncertainty sets for p and x_0 is subsequently exploited in the design of a point-based update law, in which the parameter estimate is projected onto the updated sets. The adaptive law for the point estimate is the

following projection modified normalized gradient descent-based scheme.

$$\bar{\theta}_{t+1} \triangleq \hat{\theta}_t + \frac{\kappa \mathcal{W}_{t+1}^\top (\mathcal{Y}_{t+1} - \mathcal{W}_{t+1} \hat{\theta}_t)}{1 + \text{trace}(\mathcal{W}_{t+1}^\top \mathcal{W}_{t+1})} \quad \forall t \in \mathbb{I}_0^\infty, \quad (23a)$$

$$\hat{\theta}_{t+1} = \begin{cases} \bar{\theta}_{t+1}, & \text{if } \bar{p}_{t+1} \in \Pi_{t+1} \text{ and } \bar{x}_{0,t+1} \in \mathbb{X}_{0,t+1} \\ \begin{bmatrix} \hat{p}_{t+1} \\ \hat{x}_{0,t+1} \end{bmatrix}, & \text{otherwise,} \end{cases} \quad (23b)$$

where $\kappa \in (0, 2)$,

$$\bar{p}_{t+1} \triangleq \bar{\theta}_{t+1}(1 : qn + mn, 1), \quad (24a)$$

$$\bar{x}_{0,t+1} \triangleq \bar{\theta}_{t+1}(qn + mn + 1 : qn + mn + n, 1), \quad (24b)$$

$$\hat{p}_{t+1} \triangleq \arg \min_{\zeta \in \Pi_{t+1}} \|\bar{p}_{t+1} - \zeta\|_2, \quad (24c)$$

$$\hat{x}_{0,t+1} \triangleq \arg \min_{\zeta \in \mathbb{X}_{0,t+1}} \|\bar{x}_{0,t+1} - \zeta\|_2. \quad (24d)$$

The estimates \hat{A}_{t+1} and \hat{B}_{t+1} are obtained as

$$\hat{\psi}_{t+1} = \mathcal{Z}_1^{-1}(\hat{p}_{t+1}, f, q), \quad (25a)$$

$$\hat{A}_{t+1} = \hat{\psi}_{t+1}(:, 1 : n), \quad (25b)$$

$$\hat{B}_{t+1} = \hat{\psi}_{t+1}(:, n + 1 : n + m). \quad (25c)$$

Further, since $\mathbb{X}_{0,t}$ is updated, the definition (14) is improved to

$$\tilde{\mathbb{X}}_{0,t} \triangleq \{x \mid x + \hat{x}_{0,t} \in \mathbb{X}_{0,t}\}. \quad (26)$$

The steps for implementing the observer are given in Algorithm 2.

Lemma 1: If the true parameters and initial condition of (1a) belong to the initial uncertainty sets, i.e., $p \in \Pi_0$ (or $\psi \in \Psi_0$) and $x_0 \in \mathbb{X}_{0,0}$, then they also belong to the update sets obtained using (18)-(20), i.e.,

$$p \in \Pi_t, \quad \psi \in \Psi_t, \quad x_0 \in \mathbb{X}_{0,t} \quad \forall t \in \mathbb{I}_0^\infty,$$

where the updated sets are nested, i.e.,

$$\Pi_t \subseteq \Pi_{t-1}, \quad \Psi_t \subseteq \Psi_{t-1}, \quad \mathbb{X}_{0,t} \subseteq \mathbb{X}_{0,t-1} \quad \forall t \in \mathbb{I}_1^\infty.$$

Consequently, the sets Π_t , Ψ_t , $\mathbb{X}_{0,t}$ and $\tilde{\mathbb{X}}_{0,t}$ are non-empty $\forall t \in \mathbb{I}_0^\infty$.

Proof: Refer to Appendix III. \blacksquare

For the convergence analysis, the minimal robust positive invariant (RPI) set generated as $\lim_{t \rightarrow \infty} \bigoplus_{i=0}^{t-1} F^i \mathbb{D}$ is required. To keep the computation tractable,

$$\mathbb{D}^{RPI} = \text{Outer RPI approximation of } \lim_{t \rightarrow \infty} \bigoplus_{i=0}^{t-1} F^i \mathbb{D} \quad (27)$$

is used, which can be obtained using [34]. The set \mathbb{D}^{RPI} contains all possible values of the disturbance-related summation term in (11a). Accordingly, the minimal RPI set containing η_t is $C\mathbb{D}^{RPI}$.

Theorem 1: Suppose the input u_t to the plant (1a) and the adaptive observer (12), and the output y_t in (1b) are uniformly bounded. Define an error $e_t \triangleq$

$(\mathcal{Y}_t - \mathcal{W}_t \hat{\theta}_{t-1}) / (1 + \text{trace}(\mathcal{W}_t^\top \mathcal{W}_t))$, where \mathcal{Y}_t , \mathcal{W}_t are matrices formed with (16a)-(17), (49) using the data available on system (1). The update law in (23) with (24), (25) guarantees

- (1) e_t , $e_t (1 + \text{trace}(\mathcal{W}_t^\top \mathcal{W}_t))^{1/2}$, $\hat{\theta}_t \in \mathcal{L}_\infty$,
- (2) e_t , $e_t (1 + \text{trace}(\mathcal{W}_t^\top \mathcal{W}_t))^{1/2}$, $\|\hat{\theta}_t - \hat{\theta}_{t-1}\|_2 \in \mathcal{S}(\bar{\eta}^2)$,² where $\bar{\eta}$ is the upper bound of $\|\eta(1 + \text{trace}(\mathcal{W}_t^\top \mathcal{W}_t))^{-1/2}\|_2$, and $\eta \in \mathbb{C}\mathbb{D}^{RPI}$, defined in (27).
- (3) the state estimation error $\tilde{x}_t = x_t - \hat{x}_t \in \mathcal{L}_\infty$.

Proof: The proof directly follows from [14, Lemma 1]. Note that \mathcal{W}_t is formed using C , F which are constants, and M_t whose dynamics is BIBO stable; this implies \mathcal{W}_t has a finite upper bound. Similarly, since $\sigma \in (0, 1)$ (refer to Appendix II), the worst-case set for $\eta_{t(i)}$ in (17) is $\mathbb{C}\mathbb{D}^{RPI}$, implying that $\bar{\eta}$ is a finite known constant. ■

IV. OUTPUT FEEDBACK ADAPTIVE TUBE MPC

Building on the adaptive observer framework developed earlier and motivated by [14], [15], the COCP is reformulated in terms of the quantities available at each time step: the state estimate (observer state) \hat{x}_t , its initial condition \hat{x}_{0_t} , the parameter point estimates \hat{A}_t , \hat{B}_t , and the uncertainty sets Ψ_t , \mathbb{X}_{0_t} . All COCP components are updated as these estimates evolve.

Analysis proceeds in two stages. First, the point estimate is held fixed, reducing the problem to a standard observer-based tube MPC formulation. Recursive feasibility and stability then follow from classical arguments [5], [31]–[33]. Crucially, contraction of uncertainty sets Ψ_t and \mathbb{X}_{0_t} only relaxes the constraint tightening and enlarges the feasible region; it therefore cannot invalidate a previously feasible solution. Stability and feasibility guarantees are thus preserved even as the set shrinks.

In the fully adaptive setting, however, the point estimate and consequently, the prediction model and the feasible region, may change at every sampling instant. The COCP is therefore time-varying, and the standard argument that relies on shifting the previous optimal solution forward by one step no longer applies. Recursive feasibility and stability must be established separately through a suitable backup solution.

The COCP components are first constructed for a fixed-point estimate and then extended to the fully adaptive case. Two sources of error arise in this setting: state estimation error and prediction error, as discussed in the following subsections.

A. Constraint tightening for state estimation error

Feasibility of the COCP ensures constraint satisfaction for the observer state but does not directly guarantee constraint satisfaction for the true plant state. This gap is addressed through constraint tightening based on the state estimation error dynamics. From (11a) and (12a),

$$\tilde{x}_t = M_t \tilde{p}_t + F^t \tilde{x}_{0_t} + \sum_{k=0}^{t-1} F^{t-1-k} d_k, \quad (28)$$

²A sequence vector z_t is said to belong to $\mathcal{S}(\bar{\eta}^2)$ if $\sum_{i=t}^{t+k} z_i^\top z_i \leq c_0 \bar{\eta}^2 k + c_1 \forall t \in \mathbb{I}_1^\infty$, a given constant $\bar{\eta}^2$, and some $k \in \mathbb{I}_1^\infty$, where $c_0, c_1 \geq 0$ [35, Theorem 4.11.2, footnote 6].

where $\tilde{p}_t \triangleq p - \hat{p}_t$ and $\tilde{x}_{0_t} \triangleq x_0 - \hat{x}_{0_t}$, are the parameter estimation error and initial state estimation error, respectively.

The COCP at time t uses the point estimates available at that time, which are fixed over the prediction horizon. The predicted observer state and corresponding estimation error are denoted by $\hat{x}_{t,i}$ and $\tilde{x}_{t,i}$, respectively, where $\hat{x}_{t,i}$ represents the i -step-ahead predicted observer state and $\tilde{x}_{t,i}$ the corresponding estimation error³. With fixed point estimates,

$$\hat{x}_{t,i} = M_{t+i} \hat{p}_t + F^{t+i} \hat{x}_{0_t} \quad (\text{from (12a)}), \quad (29)$$

which when subtracted from (11a) at time $t+1$ yields

$$\begin{aligned} \tilde{x}_{t,1} &= x_{t+1} - \hat{x}_{t,1} = (FM_t + [Y_t \ U_t]) \tilde{p}_t \\ &+ F^{t+1} \tilde{x}_{0_t} + \sum_{k=0}^{t-1} F^{t-k} d_k + d_t \\ \Rightarrow \tilde{x}_{t,i+1} &= F \tilde{x}_{t,i} + [Y_{t+i} \ U_{t+i}] \tilde{p}_t + d_{t+i}; \quad \tilde{x}_{t,0} = \tilde{x}_t \\ &\forall t \in \mathbb{I}_0^\infty, \quad i \in \mathbb{I}_0^{N-1}. \end{aligned} \quad (30)$$

Propagating the dynamics in (30) yields the sets $\tilde{\mathbb{X}}_{t,i} \ni \tilde{x}_{t,i}$:

$$\begin{aligned} \tilde{\mathbb{X}}_{t,i} &= F^{t+i} \tilde{\mathbb{X}}_{0_t} \oplus \bigoplus_{k=0}^{t+i-1} F^{t+i-1-k} (\mathcal{D}_{y_{u_t}} \oplus \mathbb{D}) \\ \mathcal{D}_{y_{u_t}} &\triangleq \{ [I_n \otimes y^\top \quad I_n \otimes u^\top] \tilde{p} \mid y \in C\mathbb{X}, \\ &u \in \mathbb{U}, \tilde{p} \in \Pi_t \ominus \hat{p}_t \}. \end{aligned} \quad (32)$$

Constraint sets for the state estimates are given by

$$\hat{x}_{t,i} \in \tilde{\mathbb{X}}_{t,i} \triangleq \mathbb{X} \ominus \tilde{\mathbb{X}}_{t,i}. \quad (33)$$

For the COCP to be feasible, the tightened sets $\tilde{\mathbb{X}}_{t,i}$ must be non-empty. To characterize a conservative worst-case bound on the estimation error sets $\tilde{\mathbb{X}}_{t,i}$ over the prediction horizon, define

$$\bar{\mathcal{X}}_t \triangleq F^t \tilde{\mathbb{X}}_{0_t} \oplus \mathcal{D}_{y_{u_t}}^{RPI} \oplus \mathbb{D}^{RPI}, \quad (34)$$

where $\bar{\mathcal{X}}_t \supseteq \tilde{\mathbb{X}}_{t,i}$, and

$$\mathcal{D}_{y_{u_t}}^{RPI} = \text{Outer RPI approximation of} \\ \lim_{t \rightarrow \infty} \bigoplus_{k=0}^{t-1} F^{t-1-k} \mathcal{D}_{y_{u_t}} \quad (35)$$

is obtained using [34]. Consequently, if $\mathbb{X} \ominus \bar{\mathcal{X}}_t$ is non-empty, then the tightened sets $\tilde{\mathbb{X}}_{t,i}$ also remain non-empty. Accordingly, the following standard assumption is imposed [1]–[4], [31]–[33].

Assumption 2: The set $\mathbb{X} \ominus \bar{\mathcal{X}}_0$ is non-empty. This assumption ensures that at the initial time, even after subtracting the worst-case uncertainty effects, the set \mathbb{X} retains admissible states, i.e., the tightened set remains non-empty to allow running a COCP.

Remark 2: If Assumption 2 holds and the point estimate $\hat{\theta}_t$ remains fixed, then the sets $\mathbb{X} \ominus \bar{\mathcal{X}}_t$ remain non-empty and expand monotonically with time, i.e., $\mathbb{X} \ominus \bar{\mathcal{X}}_t \supseteq \mathbb{X} \ominus \bar{\mathcal{X}}_{t-1}$ for all t (by Assumption 1). Further, for implementation purposes, Assumption 2 is verified for a fixed point estimate rather than

³The notation $(\cdot)_{t,i}$ corresponds to the case of fixed point estimates, and is used to avoid ambiguity with the actual signal $(\cdot)_{t+i}$.

over all elements of Ψ_0 which reduces conservatism. Also, $\tilde{\mathcal{X}}_0$ is a conservative bound; since the first term in $\tilde{\mathcal{X}}_{t,i}$ decreases with time and the summation terms converge, tighter bounds on $\tilde{\mathcal{X}}_{t,i}$ can be obtained at each step.

B. Constraint tightening for prediction error

The prediction model in the COCP propagates the observer state using (12a) with fixed point estimates, given by

$$\begin{aligned}\hat{x}_{t,i+1} &= M_{t+i+1}\hat{p}_t + F^{t+i+1}\hat{x}_{0_t} \\ &= (FM_{t+i} + [Y_{t+i} \ U_{t+i}])\hat{p}_t + F^{t+i+1}\hat{x}_{0_t} \\ &= F\hat{x}_{t,i} + [Y_{t+i} \ U_{t+i}]\hat{p}_t \\ &= F\hat{x}_{t,i} + (\hat{A}_t - F)x_{t+i} + \hat{B}_t u_{t+i},\end{aligned}$$

which depends on future values of the true state x_{t+i} that are not available. To eliminate this dependence, the dynamics is rewritten in terms of available quantities as

$$\hat{x}_{t,i+1} = \hat{A}_t \hat{x}_{t,i} + \hat{B}_t u_{t+i} + \underbrace{(\hat{A}_t - F)\tilde{x}_{t,i}}_{\varepsilon_{t,i}}, \quad (36)$$

which is used for state prediction within the COCP. The term $\varepsilon_{t,i}$ represents the mismatch between the prediction model and the observer dynamics, and is referred to as the *prediction error*, where

$$\varepsilon_{t,i} \in \mathcal{E}_{t,i} \triangleq (\hat{A}_t - F)\tilde{\mathcal{X}}_{t,i}. \quad (37)$$

This error is treated as a lumped disturbance within a robust homothetic tube-based MPC framework.

Unlike [10], [14], [15], where the prediction error bounds grow with the horizon length N to account for the unavailability of future parameter estimates, in the present formulation, the point estimates are held fixed over the prediction horizon. As a result, $\mathcal{E}_{t,i}$ is independent of N , which reduces conservatism and removes the restriction on the horizon length.

C. Terminal set construction

The terminal set is chosen as the maximal admissible RPI set for the prediction dynamics in (36) with respect to the prediction error $\mathcal{E}_{t,N-1}$ for $t \in \mathbb{I}_0^\infty$. This maximizes the terminal region and reduces the control effort required to steer the observer state into it, potentially allowing shorter horizons and fewer decision variables. The worst-case prediction error at the terminal step is

$$\bar{\mathcal{E}}_t \triangleq (\hat{A}_t - F) \left(F^{t+N-1} \tilde{\mathcal{X}}_{0_t} \oplus \mathfrak{D}_{y_{u_t}}^{RPI} \oplus \mathbb{D}^{RPI} \right), \quad (38)$$

and the tightened terminal constraint set is

$$\mathcal{X}_t \triangleq \mathbb{X} \ominus \left(F^{t+N} \tilde{\mathcal{X}}_{0_t} \oplus \mathfrak{D}_{y_{u_t}}^{RPI} \oplus \mathbb{D}^{RPI} \right). \quad (39)$$

To ensure feasibility and stability, the terminal set $\hat{\mathcal{X}}_{TS_t}$ at initialization ($t = 0$) is constructed under the following standard assumption [1]–[6], [8]–[15], [17]–[19], [31]–[33].

Assumption 3: For any $[\hat{A}_0 \ \hat{B}_0] \in \Psi_0$, and the pair (P_0, K_0) computed using (4) with $Q, R \succ 0$, there exists

a non-empty terminal set $\hat{\mathcal{X}}_{TS_0}$ containing the origin in its interior such that

$$\begin{aligned}\hat{\mathcal{X}}_{TS_0} &\subseteq \mathcal{X}_0, \quad K_0 \hat{\mathcal{X}}_{TS_0} \subseteq \mathbb{U}, \\ (\hat{A}_0 + \hat{B}_0 K_0) \hat{\mathcal{X}}_{TS_0} \oplus \bar{\mathcal{E}}_0 &\subseteq \hat{\mathcal{X}}_{TS_0}.\end{aligned} \quad (40)$$

When the point estimate $\hat{\theta}_t$ is updated, the terminal ingredients P_t and K_t and the terminal set must be recomputed. Such updates may compromise stability and feasibility⁴. While Assumption 3 can be verified offline, additional conditions are required to ensure safe online switching to new point estimates. To this end, the following criterion is checked $\forall t \in \mathbb{I}_1^\infty$.

Criterion 1: Given $\hat{A}_t, \hat{B}_t, (P_{t-1}, K_{t-1}), Q, R \succ 0$, and sets $\mathcal{X}_t, \mathbb{U}, \bar{\mathcal{E}}_t$, select (P_t, K_t) with $P_t \succ 0$ such that

$$\begin{aligned}(a) \quad &P_t - (\hat{A}_t + \hat{B}_t K_t)^\top P_t (\hat{A}_t + \hat{B}_t K_t) \\ &\quad - Q - K_t^\top R K_t \succeq 0,\end{aligned} \quad (41a)$$

$$\begin{aligned}(b) \quad &P_{t-1} - (\hat{A}_t + \hat{B}_t K_t)^\top P_t (\hat{A}_t + \hat{B}_t K_t) \\ &\quad - Q - K_{t-1}^\top R K_{t-1} \succeq 0,\end{aligned} \quad (41b)$$

$$(c) \quad \left. \begin{aligned} &\hat{\mathcal{X}}_{TS_t} \subseteq \mathcal{X}_t, \quad K_t \hat{\mathcal{X}}_{TS_t} \subseteq \mathbb{U}, \\ &(\hat{A}_t + \hat{B}_t K_t) \hat{\mathcal{X}}_{TS_t} \oplus \bar{\mathcal{E}}_t \subseteq \hat{\mathcal{X}}_{TS_t} \end{aligned} \right\} \quad (41c)$$

where $\hat{\mathcal{X}}_{TS_t}$ is non-empty and contains the origin in its interior.

Conditions (41a) and (41c) are standard terminal set requirements and can be verified offline. Condition (41b) is the key adaptive ingredient—it enforces compatibility between consecutive point estimate updates by ensuring the Lyapunov function remains non-increasing along closed-loop trajectories despite changes in the prediction model, thereby maintaining stability.

Condition (41b) is less restrictive than the quadratic stabilizability condition [20], which requires a common (P, K) for all $[\hat{A} \ \hat{B}] \in \Psi_0$; here, only consistency between successive estimates is enforced, avoiding the need for a single Lyapunov function over the entire uncertainty set.

If Criterion 1 cannot be satisfied, the point estimate is held fixed while the uncertainty sets are updated. This preserves both feasibility and stability, while still allowing reduction of uncertainty as new data becomes available.

D. Tube parameterization

At each time t , the COCP is solved using a homothetic tube-based approach [4], [5]. Two tubes are constructed: one for the observer state and the other for the control input. The geometry of the state tube-sections is defined by a polytope \mathbb{G}_t , designed based on the following standard assumption [5], [10], [12], [14], [15].

Assumption 4: The set $\mathbb{G}_t \triangleq \text{co} \left(\left\{ \mathfrak{g}_t^{[j]} \right\}_{j=1:H_t} \right) \subseteq \mathbb{R}^n$, with $H_t > 0$ known vertices, is a polytope containing the origin in its interior and satisfying

$$(\hat{A}_t + \hat{B}_t K_t) \mathbb{G}_t \oplus \hat{\mathcal{E}}_t \subseteq \mathbb{G}_t, \quad (42a)$$

$$\text{where } \hat{\mathcal{E}}_t \triangleq (\hat{A}_t - F) \bar{\mathcal{X}}_t. \quad (42b)$$

⁴Recursive feasibility may be affected for small prediction horizons or empty tightened constraints; this is discussed later in Sec. IV-F.

For a given t and prediction horizon N , $F^t \tilde{\mathbb{X}}_{0_t} \supseteq F^{t+i} \tilde{\mathbb{X}}_{0_t}$ for all $i \in \mathbb{I}_0^N$ (by Assumption 1), while $\mathcal{D}_{y_{u_t}}^{RPI} \oplus \mathbb{D}^{RPI}$ captures all possible values of the summation terms in (31). These imply that \mathbb{G}_t is RPI for the prediction dynamics in (36) with respect to all admissible values of prediction error $\varepsilon_{t,i}$. In practice, \mathbb{G}_t is chosen as the minimal RPI set, computed using [34], to capture the worst-case prediction error.

The observer state and control input tubes are defined as

$$\mathcal{T}_t^{\hat{x}} \triangleq \left\{ \mathbb{T}_{i|t}^{\hat{x}} \right\}_{i=0:N}, \quad \mathcal{T}_t^u \triangleq \left\{ \mathbb{T}_{i|t}^u \right\}_{i=0:N-1}, \quad (43a)$$

$$\mathbb{T}_{i|t}^{\hat{x}} = \text{co} \left(\left\{ \mathfrak{s}_{i|t}^{[j]} \right\}_{j=1:H_t} \right) \triangleq \alpha_{i|t} \oplus \beta_{i|t} \mathbb{G}_t, \quad (43b)$$

$$\Rightarrow \mathfrak{s}_{i|t}^{[j]} \triangleq \alpha_{i|t} + \beta_{i|t} \mathfrak{g}_t^{[j]}, \quad (43c)$$

$$\mathbb{T}_{i|t}^u = \left\{ \mathbb{u}_{i|t}^{[j]} \right\}_{j=1:H_t}. \quad (43d)$$

For any point $s \in \mathbb{T}_{i|t}^{\hat{x}}$, expressed as $s = \sum_{j=1}^{H_t} \tau_{(i,t)}^{[j]} \mathfrak{s}_{i|t}^{[j]}$, where each $\tau_{(i,t)}^{[j]} \in [0, 1]$ and $\sum_{j=1}^{H_t} \tau_{(i,t)}^{[j]} = 1$, the control input is generated by the same convex combination of control vertices as follows:

$$u = \mathcal{Z}_2(s, \mathbb{T}_{i|t}^{\hat{x}}, \mathbb{T}_{i|t}^u) \triangleq \sum_{j=1}^{H_t} \tau_{(i,t)}^{[j]} \mathbb{u}_{i|t}^{[j]}. \quad (44)$$

E. Reformulated COCP

Let $\mu_t \triangleq \left\{ \left\{ (\alpha_{i|t}, \beta_{i|t}) \right\}_{i=0:N}, \left\{ \mathbb{u}_{i|t}^{[j]} \right\}_{i=0:N-1, j=1:H_t} \right\}$ denote the decision variable. The COCP is given by

$$\mathbb{P}_t : \min_{\mu_t} \sum_{j=1}^{H_t} \left(\sum_{i=0}^{N-1} \left(\|\mathfrak{s}_{i|t}^{[j]}\|_Q^2 + \|\mathbb{u}_{i|t}^{[j]}\|_R^2 \right) + \|\mathfrak{s}_{N|t}^{[j]}\|_{P_t}^2 \right) \quad (45a)$$

subject to (41) – (43),

$$\beta_{i|t} \geq 0 \quad \forall i \in \mathbb{I}_1^N, \quad (45b)$$

$$\hat{x}_t \in \mathbb{T}_{0|t}^{\hat{x}}, \quad (45c)$$

$$\mathbb{T}_{i|t}^{\hat{x}} \subseteq \tilde{\mathbb{X}}_{t,i}, \quad \mathbb{T}_{i|t}^u \subseteq \mathbb{U} \quad \forall i \in \mathbb{I}_0^{N-1}, \quad (45d)$$

$$\mathbb{T}_{N|t}^{\hat{x}} \subseteq \tilde{\mathbb{X}}_{T,s_t}, \quad (45e)$$

$$\hat{A}_t \mathfrak{s}_{i|t}^{[j]} + \hat{B}_t \mathbb{u}_{i|t}^{[j]} \in \mathbb{T}_{i+1|t}^{\hat{x}} \ominus \mathcal{E}_{t,i} \quad \forall (i, j) \in \mathbb{I}_0^{N-1} \times \mathbb{I}_1^{H_t}. \quad (45f)$$

The input applied to the plant (1a) and observer (12) is obtained from the optimal solution using (44), i.e.,

$$u_t^* = \mathcal{Z}_2(\hat{x}_t, \mathbb{T}_{0|t}^{\hat{x}*}, \mathbb{T}_{0|t}^{u*}).$$

At time $t+1$, a new COCP is constructed using the updated sets Ψ_{t+1} , $\mathbb{X}_{0_{t+1}}$ and estimates \hat{A}_{t+1} , \hat{B}_{t+1} . This transition requires additional conditions to preserve stability and recursive feasibility. As subsequently shown in Theorem 3, stability is ensured if condition (41b) holds. However, even when Criterion 1 is satisfied, infeasibility of (45) may arise due to a short prediction horizon or empty tightened sets $\tilde{\mathbb{X}}_{t+1,i}$. To address this, a fallback mechanism is employed by reverting

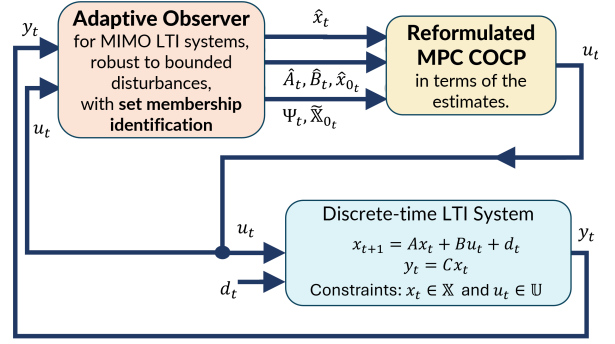


Fig. 1. Schematic diagram for the proposed adaptive tube MPC.

to the previous estimates:

$$\begin{aligned} \hat{x}_{0_{t+1}} &\leftarrow \hat{x}_{0_t}, \quad \hat{A}_{t+1} \leftarrow \hat{A}_t, \quad \hat{B}_{t+1} \leftarrow \hat{B}_t, \quad P_{t+1} \leftarrow P_t, \\ K_{t+1} &\leftarrow K_t, \quad \Psi_{t+1} \leftarrow \text{co}(\Psi_{t+1}, \{[\hat{A}_t \quad \hat{B}_t]\}), \\ \Pi_{t+1} &\leftarrow \text{co}(\Pi_{t+1}, \{\hat{p}_t\}), \quad \mathbb{X}_{0_{t+1}} \leftarrow \text{co}(\mathbb{X}_{0_{t+1}}, \{\hat{x}_{0_t}\}). \end{aligned} \quad (46)$$

The observer state is then recomputed using (12a), and the COCP components are reconstructed as described in Sec. IV, after which the COCP is solved at time $t+1$.

Any update to Ψ_t , \mathbb{X}_{0_t} , or the estimates \hat{A}_t , \hat{B}_t , \hat{x}_t , \hat{x}_{0_t} modifies the geometry of the sets involved in the COCP, including the polytope \mathbb{G}_t , yielding an *adaptive tube*, enabling improved characterization of uncertainty in the propagation of both the observer state and the true plant state. The implementation steps are summarized in Algorithm 1, and the proposed scheme is illustrated in Fig. 1.

Remark 3: The number of vertices of Ψ_t and \mathbb{X}_{0_t} may grow with time. To preserve computational tractability, the adaptation of the sets can be halted once the number of vertices L_{p_t} and L_{x_t} reach prescribed upper bounds determined by the available computational resources. Alternatively, complexity-management techniques such as those proposed in [3], [12], [37] may be employed.

Remark 4: Computing all the sets of Sec. IV and running the COCP again at $t \leftarrow t+1$ can be time-consuming. An alternative is to reuse the control input obtained from the previous step: $u_t = \mathcal{Z}_2(\hat{x}_t, \mathbb{T}_{1|t-1}^{\hat{x}*}, \mathbb{T}_{1|t-1}^{u*})$, along with the modified setup (46).

Remark 5: In computing $\tilde{\mathbb{X}}_{t,i}$ using (31), the set $\mathcal{D}_{y_{u_t}}$ consists of a component involving \tilde{p}_t that is constant across the prediction horizon at any given time t . This component, along with the accumulated disturbance terms $\bigoplus_{k=0}^{t-1-k} F^{t-1-k} \mathbb{D}$ and $\mathcal{D}_{y_{u_t}}^{RPI}$, can be updated recursively across time steps, avoiding full recomputation at each t .

F. Recursive feasibility and stability analysis

Theorem 2: Consider the system (1) subject to the constraints (2) for which Assumptions 1-4 hold, and the adaptive observer that provides point estimates and updated sets using (12)-(25), (49). If the COCP \mathbb{P}_t is feasible, then \mathbb{P}_{t+k} is also feasible $\forall k \in \mathbb{I}_1^\infty$.

Proof: Refer to Appendix IV. ■

Algorithm 1 Output Feedback MPC with Adaptive Tubes

Input: $\mathbb{X}, \mathbb{U}, \mathbb{D}, \psi^{[i]} \forall i \in \mathbb{I}_1^{L_{p0}}$ and $\hat{\psi}_0$ with P_0, K_0 satisfying (4) for ψ_0, F , the L_{x_0} vertices of \mathbb{X}_0 and \hat{x}_{0_0} such that Assumption 1 holds, N, Q, R, κ, σ .

Output: The optimal decision variable $\mu_t^* \forall t \in \mathbb{I}_0^\infty$.

```

1: Initialize the sets  $\Psi_0 = \Psi, \mathbb{X}_{0_0} = \mathbb{X}_0$ , a constant  $c_{backup} = 0$  and time  $t = 0$ .
2: Compute  $\mathbb{D}^{RPI}$  using (27) and [34].
3: Measure  $y_0$ .
4: while  $t \geq 0$  do
5:   Compute the following using the references given in parentheses:  $\Pi_t$  [(9)],  $\hat{\theta}_t$  [(12b)],  $\mathbb{X}_{0_t}$  [(26)],  $\mathbb{X}_{t,i}$  [(31)] and  $\hat{\mathbb{X}}_{t,i}$  [(33)]  $\forall i \in \mathbb{I}_0^N, \mathcal{D}_{y_{u_t}}$  [(32)],  $\mathcal{D}_{y_{u_t}}^{RPI}$  [(35)],  $\mathcal{E}_{t,i}$  [(37)],  $\hat{\mathcal{E}}_t$  [(38)],  $\hat{\mathcal{E}}_t$  [(42b)],  $\mathbb{G}_t$  [Assumption 4 using [34]].5
6:   if  $t == 0$  then
7:     Compute  $\hat{\mathbb{X}}_{TS_t}$  satisfying (40) using [36].
8:   else
9:     Check if  $\exists P_t, K_t$  and  $\hat{\mathbb{X}}_{TS_t}$  (computed using [36]) satisfying Criterion 1.
10:    if Criterion 1 does not hold then
11:      Set  $c_{backup} \leftarrow 1$  and  $t \leftarrow t - 1$ , and go to Step 29.
12:    end if
13:  end if
14:  Run the COCP  $\mathbb{P}_t$  in (45).
15:  if (45) is feasible, i.e.,  $\mu_t^* \neq \emptyset$  then
16:    Set  $c_{backup} \leftarrow 0$ .
17:  else
18:    if  $t == 0$  then
19:      Print 'Initially infeasible setup', and exit the algorithm.
20:    else
21:      Set  $c_{backup} \leftarrow 1$  and  $t \leftarrow t - 1$ .
22:    end if
23:  end if
24:  if  $c_{backup} == 0$  then
25:    Apply  $u_t^*$  computed using (44) to the true system and measure  $y_{t+1}$ .
26:    Apply  $u_t^*, y_t$  and  $y_{t+1}$  to the adaptive observer.
27:    Obtain  $\Psi_{t+1}, \mathbb{X}_{0_{t+1}}, \hat{A}_{t+1}, \hat{B}_{t+1}, \hat{x}_{0_{t+1}}$  and  $\hat{x}_{t+1}$  using Algorithm 2.
28:  end if
29:  if  $c_{backup} == 1$  then
30:    Obtain the point estimates and uncertainty sets using (46).
31:  end if
32:  Update  $t \leftarrow t + 1$ .
33: end while

```

Theorem 3: Provided Assumptions 1-4 hold for system (1) subject to the constraints (2), and the COCP \mathbb{P}_t at $t = 0$ is feasible, then, under Algorithms 1 and 2, the following are guaranteed.

(1) The signals $x_t, \hat{x}_t, u_t, \hat{\theta}_t \in \mathcal{L}_\infty$.

⁵For $t = 0$, Steps 5 and 7 may be performed offline.

Algorithm 2 Adaptive Observer

Input: $t, F, C, \hat{\psi}_t, \hat{x}_{0_t}, u_t, y_t, y_{t+1}, q, n, m$.

Output: $\Psi_{t+1}, \mathbb{X}_{0_{t+1}}, \hat{A}_{t+1}, \hat{B}_{t+1}, \hat{x}_{0_{t+1}}, \hat{x}_{t+1}$.

```

1: Compute  $M_{t+1}$  using (10),  $\omega_{t+1}$  and  $\hat{\theta}_{t+1}$  using (12b), and  $\mathcal{Y}_{t+1}, \mathcal{W}_{t+1}, \mathcal{N}_{t+1(i)}$   $\forall i \in \mathbb{I}_0^{qn+mn+n-1}$  using (16a)-(17), (49).
2: Compute  $\Xi_{t+1}$  using (18).
3: Update  $\Pi_{t+1}, \mathbb{X}_{0_{t+1}}$  and  $\Psi_{t+1}$  with (19) and (20).
4: Update  $\hat{p}_{t+1}$  and  $\hat{x}_{0_{t+1}}$  using (23), (24).
5: Obtain  $\hat{A}_{t+1}, \hat{B}_{t+1}$  from (25), and  $\hat{x}_{t+1}$  from (12a).

```

(2) The adaptive observer exhibits robust exponential stability, i.e., \exists constants $c_1 > 0, c_2 \in (0, 1)$ such that

$$\|\hat{x}_t\| \leq c_1 c_2^t \|\hat{x}_0\| + c_3 \quad \forall t \in \mathbb{I}_0^\infty,$$

for some bounded constant c_3 depending on the disturbance, state estimation error and prediction error bounds. Further, the state estimation error sets are uniformly bounded implying the actual plant also exhibits robust exponential stability.

Proof: The proof for $x_t, \hat{x}_t, u_t, \hat{\theta}_t \in \mathcal{L}_\infty$ easily follows due to constraint tightening and recursive feasibility of the COCP, by Theorem 2, and the observer properties guaranteed by Lemma 1 and Theorem 1.

For the proof of the second part, refer to Appendix V. ■

Remark 6: The overall scheme is initialized with user-specified estimates, rather than through the observer in Algorithm 2. These are used in Algorithm 1 to solve the COCP and obtain the optimal decision variable μ_t^* . The resulting input is then applied to the system to obtain the next output; the corresponding measurements are supplied to the observer to produce updated estimates via Algorithm 2. This ensures that the conditions of uniformly bounded input and output, as required for observer convergence using Theorem 1, are met from the outset.

Theorem 4: When no adaptation is performed, i.e., the point estimate $\hat{\theta}_t$ and the uncertainty sets Π_t, Ψ_t and \mathbb{X}_{0_t} are held fixed, the resulting closed-loop scheme reduces to a Luenberger observer-based output feedback tube MPC where the parametric uncertainty is treated as an additive disturbance, without any loss of recursive feasibility, robustness and stability guarantees for the COCP \mathbb{P}_t .

Proof: Refer to Appendix VI. ■

V. SIMULATION RESULTS AND DISCUSSION

A second-order LTI system⁶ is considered:

$$\begin{aligned} x_{t+1} &= \begin{bmatrix} -1.2 & 1 \\ 0.2 & 0 \end{bmatrix} x_t + \begin{bmatrix} 4 \\ -3.233 \end{bmatrix} u_t + d_t, \\ y_t &= [1 \quad 0] x_t, \end{aligned}$$

subject to constraints $\|x_t\|_\infty \leq 40, \|u_t\|_\infty \leq 4$, disturbance bound $\|d_t\|_\infty \leq 0.1$, and parametric uncertainty set $\Psi_0 =$

⁶A second-order system is considered to facilitate visualization of the tube geometry.

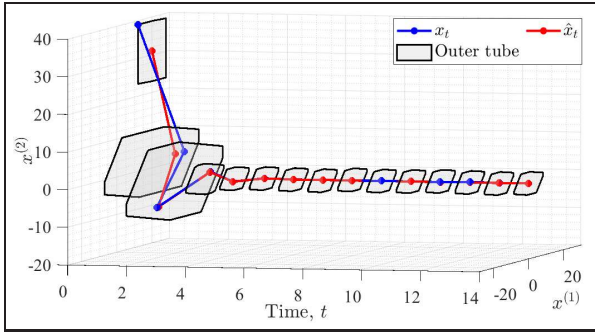


Fig. 2. True state and state estimate trajectories, with the outer tube (in grey) guaranteed to contain the true state trajectory.

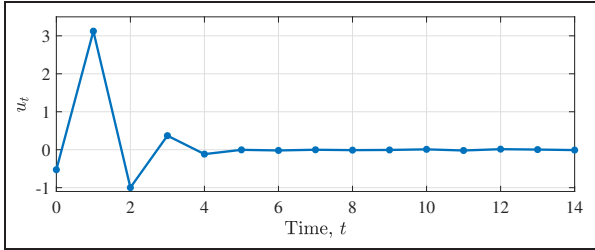


Fig. 3. Control input.

$\text{co} \left(\left\{ \psi_0^{[i]} \right\}_{i=1:3} \right)$ ⁷. The initial set \mathbb{X}_0 is shown in grey in Fig. 8 (b). The COCP is implemented with horizon $N = 10$, weights $Q = I_2$, $R = 0.1$, and observer parameters $\kappa = 0.2$, and $\sigma = 0.9$. The true and observer initial states are chosen as

$$x_0 = \begin{bmatrix} 12 \\ 39 \end{bmatrix}, \quad \hat{x}_0 = \begin{bmatrix} 20 \\ 31 \end{bmatrix}, \quad \text{with } F = \begin{bmatrix} 0.03 & 1 \\ 0.01 & 0 \end{bmatrix}.$$

The trajectories of the true and observer states, and control input are shown in Figs. 2 and 3, respectively. The state tube-sections in Fig. 2, given by $\hat{x}_t \oplus \mathbb{T}_{0|t}^{\hat{x}}$, enclose the true state trajectory at all times while satisfying the imposed state constraint. The input constraint is also satisfied.

The adaptation of the tubes $\mathcal{T}_t^{\hat{x}}$ for the state estimate is illustrated in Fig. 4 for $t = 0$ to $t = 3$. Convergence of both the state and observer state trajectories to neighbourhoods of the origin is observed, along with decay of the input (see Figs. 2, 3). The first two tube-sections returned by the COCP at previous time instant are shown in the background in the last three sub-figures of Fig. 4; the tube size visibly reduces with adaptation, giving a better characterization of the uncertainty in propagation of observer dynamics. The changes in the tube geometry are shown in Fig. 5.

It is worth noting that the state estimate at $t = 1$ is not contained in the tube-section $\mathbb{T}_{1|0}^{\hat{x}}$ (zoomed in first sub-figure of 4). This is expected; the yellow tube was generated under a fixed point estimate, whereas the state estimate is updated based on the improved uncertainty sets and point estimates of \hat{p}_t and $\hat{x}_{0,t}$. To illustrate this effect, the first sub-figure

⁷The vertices of Ψ_0 are $\psi_0^{[1]} = \begin{bmatrix} -1.1 & 1 & 4 \\ 0.2 & 0 & -3.1 \end{bmatrix}$, $\psi_0^{[2]} = \begin{bmatrix} -1.2 & 1 & 4 \\ 0.2 & 0 & -3 \end{bmatrix}$, and $\psi_0^{[3]} = \begin{bmatrix} -1.3 & 1 & 4 \\ 0.2 & 0 & -3.6 \end{bmatrix}$.

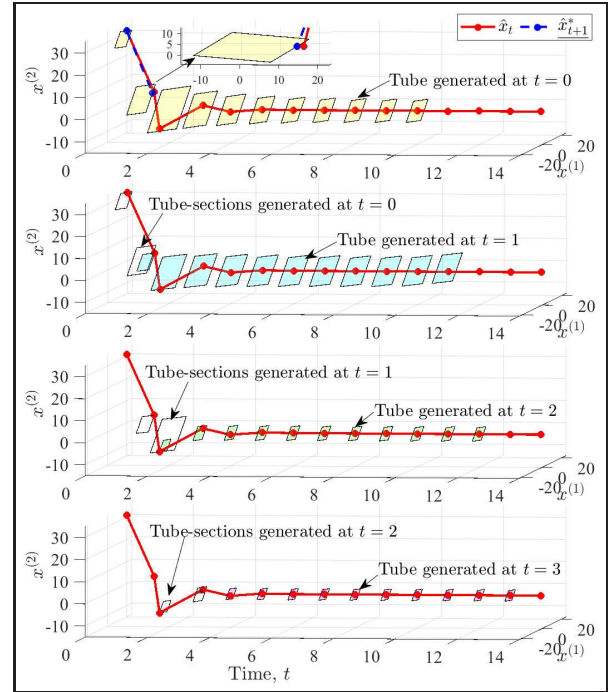


Fig. 4. Tube for state estimate trajectory generated by the COCP at $t = 0, 1, 2, 3$, in yellow, cyan, green and pink, respectively.

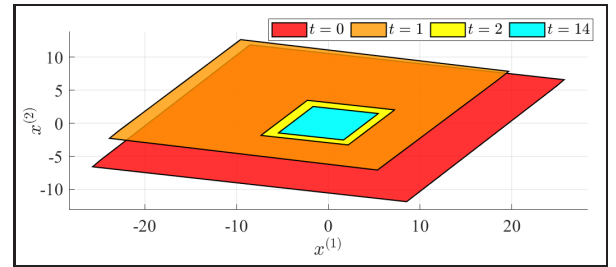


Fig. 5. The polytopes forming the tube cross-sectional shape at time t .

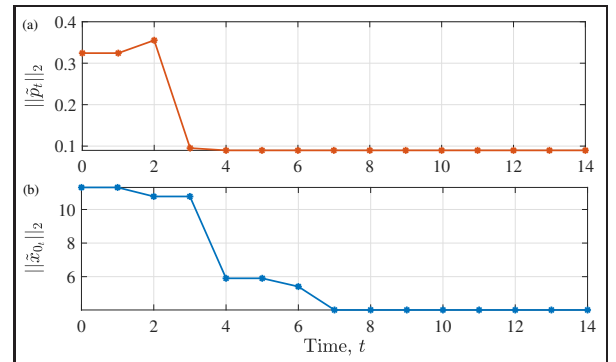


Fig. 6. Norms of the parameter estimation error and the initial state estimation error.

additionally shows, using the blue dashed line (\cdot), the state estimate trajectory obtained when the point estimates are held fixed. As expected, this trajectory remains contained within the tube-section $\mathbb{T}_{1|0}^{\hat{x}}$.

The parameter and state estimation error norms $\|\tilde{p}_t\|_2$ and $\|\tilde{x}_{0,t}\|_2$, and the associated variations in K_t and P_t are

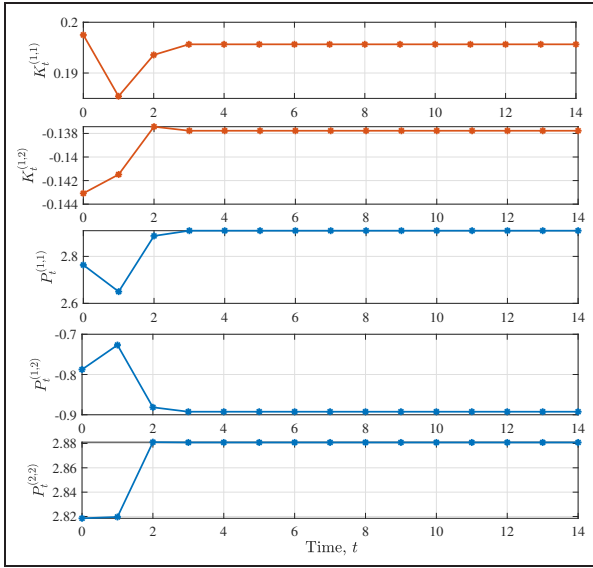


Fig. 7. Variation of the elements of the stabilizing feedback gain K_t , and the terminal cost weight P_t .

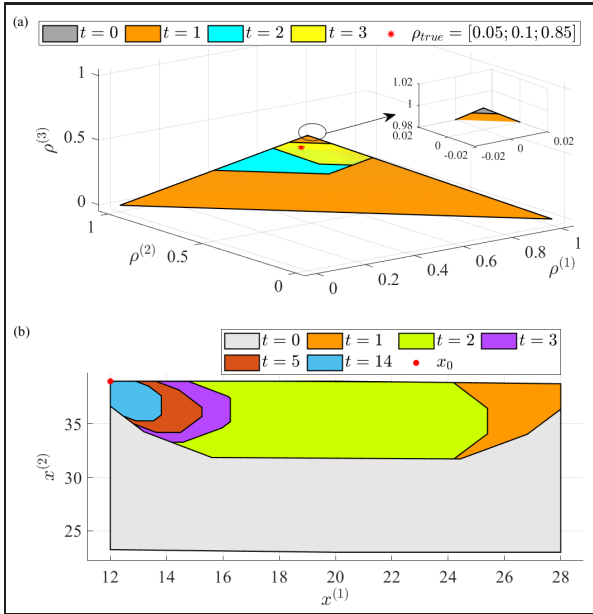


Fig. 8. Reduction in size of uncertainty sets: (a) Barycentric representation of the sets Ψ_t containing the true parameter combination $[0.05; 0.1; 0.85]$, using $\rho^{(i)}$. (b) Sets $\mathbb{X}_{0,t}$ containing the initial true state x_0 .

displayed in Figs. 6 and 7, respectively. The contraction of the uncertainty sets Ψ_t and $\mathbb{X}_{0,t}$ with time are shown in Fig. 8 (a) and (b), respectively, with Fig. 8 (a) giving a barycentric representation using $\rho^{(i)}$ for $\psi_0^{[2]}$, for ease in visualization. Both the parameter estimation norm and the uncertainty set sizes Ψ_t and $\mathbb{X}_{0,t}$ decrease with incoming data⁸. Notably, the modification of the regressors in (49) enables learning of the set $\mathbb{X}_{0,t}$ beyond $t = 2$.

A comparison with the non-adaptive case and [31] is pro-

⁸An improved convergence may be achieved with a persistently exciting regressor. Incorporating excitation constraints on the COCP has been explored in [13], [38].

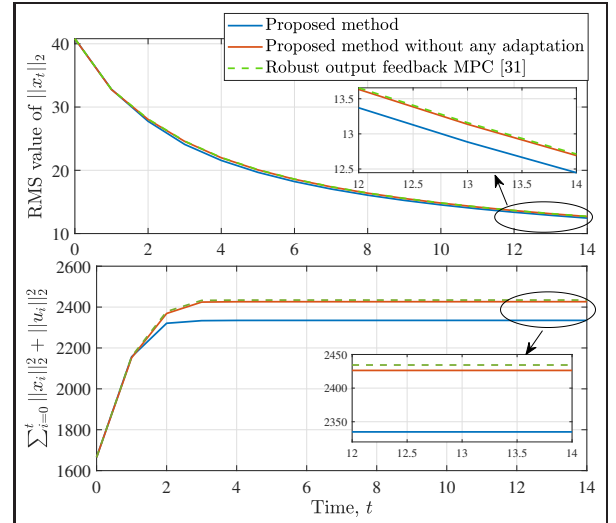


Fig. 9. Comparison of RMS value of $\|x_t\|_2$ and the cumulative stage cost for the proposed method with and without any adaptation and [31].

vided in Fig. 9, where the RMS value of $\|x_t\|_2$ and cumulative stage cost are shown. Improved performance is observed for the proposed adaptive scheme once sufficient learning has occurred. In the absence of adaptation, comparable performance with [31] is observed, consistent with Theorem 4.

VI. CONCLUSION

An adaptive observer-based output feedback MPC framework with adaptive tubes has been developed for discrete-time LTI systems subject to parametric and additive uncertainties. Point and set estimates of the unknown parameters and initial state are obtained using an adaptive observer with joint set membership-based identification, enabling progressive refinement of uncertainty descriptions. The resulting scheme induces adaptation in the tube geometry and associated sets, thereby rendering the tube an adaptive nature. As uncertainty contracts with data, constraint tightening relaxes progressively, yielding improved closed-loop performance without sacrificing guarantees.

Recursive feasibility, robust exponential stability, and boundedness of all closed-loop signals are established for the resulting time-varying COCP. Crucially, these guarantees are obtained without requiring a common quadratically stabilizing linear feedback gain over the entire uncertainty set; a compatibility condition on successive terminal ingredients, together with a backup mechanism, suffices. In the limiting case of no adaptation, the framework recovers a standard Luenberger observer-based tube MPC.

The result establishes a pathway from set membership identification to certified adaptive predictive control under output feedback. Future work will focus on reducing the computational complexity associated with online updates and extending the framework to a more general class of systems.

APPENDIX I BIJECTIVE MAPPING BETWEEN MATRIX AND VECTOR PARAMETERIZATIONS

The bijection \mathcal{Z}_1 is defined as

$$\mathcal{Z}_1 : \mathbb{R}^{n \times (n+m)} \times \mathbb{R}^{qn} \times \mathbb{I}_1^\infty \rightarrow \mathbb{R}^{qn+mn}$$

$$(\bar{\psi}, f, q) \mapsto \begin{bmatrix} \mathbf{vec}(\bar{\psi}(:, 1 : q)) - f \\ \mathbf{vec}(\bar{\psi}(:, n+1 : n+m)) \end{bmatrix}, \quad (47)$$

i.e., $\mathcal{Z}_1([A \ B], f, q) = p$, and its inverse is

$$\mathcal{Z}_1^{-1} : \mathbb{R}^{qn+mn} \times \mathbb{R}^{qn} \times \mathbb{I}_1^\infty \rightarrow \mathbb{R}^{n \times (n+m)}$$

$$(\bar{p}, f, q) \mapsto \begin{bmatrix} \bar{A} & I_{n-q} \\ 0_{q \times (n-q)} & \bar{B} \end{bmatrix}, \quad (48a)$$

$$\text{where } \bar{A} \triangleq \mathbf{vec}^{-1}(\bar{p}(1 : qn, 1) + f, n), \quad (48b)$$

$$\bar{B} \triangleq \mathbf{vec}^{-1}(\bar{p}(qn+1 : qn+mn, 1), n). \quad (48c)$$

APPENDIX II RECURSIVE CONSTRUCTION OF THE AUGMENTED REGRESSION USED BY THE ADAPTIVE OBSERVER

The detailed recursive construction of the augmented regression signals and associated uncertainty sets used in Sec. III-B are given below.

$$\omega_{0(i)} \triangleq 0_{q \times (qn+mn+n)} \quad \forall i \in \mathbb{I}_1^{qn+mn+n-1}, \quad (49a)$$

$$\omega_{t(0)} \triangleq \omega_t \quad \forall t \in \mathbb{I}_0^\infty, \quad (49b)$$

$$\omega_{t(i)} \triangleq \sigma \omega_{t-1(i)} + (1-\sigma) \omega_{t-1(i-1)} \\ \forall (t, i) \in \mathbb{I}_1^\infty \times \mathbb{I}_1^{qn+mn+n-1}, \quad (49c)$$

$$y_{0(i)} \triangleq 0_q \quad \forall i \in \mathbb{I}_1^{qn+mn+n-1}, \quad (49d)$$

$$y_{t(0)} \triangleq y_t \quad \forall t \in \mathbb{I}_0^\infty, \quad (49e)$$

$$y_{t(i)} \triangleq \sigma y_{t-1(i)} + (1-\sigma) y_{t-1(i-1)} \\ \forall (t, i) \in \mathbb{I}_1^\infty \times \mathbb{I}_1^{qn+mn+n-1}, \quad (49f)$$

$$\mathcal{N}_{0(i)} \triangleq \{0\} \quad \forall i \in \mathbb{I}_0^{qn+mn+n-1}, \quad (49g)$$

$$\mathcal{N}_{t(0)} \triangleq \bigoplus_{k=0}^{t-1} CF^{t-1-k} \mathbb{D} \quad \forall t \in \mathbb{I}_1^\infty, \quad (49h)$$

$$\mathcal{N}_{t(i)} \triangleq \sigma \mathcal{N}_{t-1(i)} \oplus (1-\sigma) \mathcal{N}_{t-1(i-1)} \\ \forall (t, i) \in \mathbb{I}_1^\infty \times \mathbb{I}_1^{qn+mn+n-1}, \quad (49i)$$

with $\sigma \in (0, 1)$.

APPENDIX III PROOF OF LEMMA 1

The matrices \mathcal{Y}_t and \mathcal{W}_t are constructed using data measured from the system (1). Consequently, the true quantities p and x_0 satisfy

$$y_{t(i)} - \omega_{t(i)} [p^\top \ x_0^\top]^\top \in \mathcal{N}_{t(i)} \quad \forall (t, i) \in \mathbb{I}_0^\infty \times \mathbb{I}_0^{qn+mn+n-1}.$$

From the definition of the non-falsified set in (18), it follows that

$$(p, x_0) \in \Xi_t \quad \forall t \in \mathbb{I}_1^\infty. \quad (50)$$

The uncertainty sets are updated through intersection as defined in (19). Hence, the updated sets are nested and satisfy

$$\Pi_t \times \mathbb{X}_{0_t} \subseteq \Pi_{t-1} \times \mathbb{X}_{0_{t-1}} \quad \forall t \in \mathbb{I}_1^\infty.$$

Since $(p, x_0) \in \Pi_0 \times \mathbb{X}_{0_0}$ and (50) holds, it follows by induction that

$$(p, x_0) \in \Pi_t \times \mathbb{X}_{0_t} \quad \forall t \in \mathbb{I}_0^\infty \\ \Rightarrow \psi \in \Psi_t, \quad p \in \Pi_t, \quad x_0 \in \mathbb{X}_{0_t}, \quad \forall t \in \mathbb{I}_0^\infty, \\ \Rightarrow \Psi_t \neq \emptyset, \quad \Pi_t \neq \emptyset, \quad \mathbb{X}_{0_t} \neq \emptyset \quad \forall t \in \mathbb{I}_0^\infty.$$

Finally, the update law in (23), (24) ensures that the estimate \hat{x}_{0_t} is projected onto \mathbb{X}_{0_t} . As a result, the set $\tilde{\mathbb{X}}_{0_t} = \mathbb{X}_{0_t} \ominus \hat{x}_{0_t}$ is non-empty for all $t \in \mathbb{I}_0^\infty$.

APPENDIX IV PROOF OF THEOREM 2

The proof proceeds by induction. Assume that the COCP (45) is feasible at time t . It is shown that feasibility is preserved at time $t+1$.

Given a feasible solution at time t , the system evolves and the point estimates and uncertainty sets are updated. Criterion 1 is then evaluated at time $t+1$. If Criterion 1 holds, a new COCP is formulated with an updated terminal cost, terminal set, and feedback gain. Since the problem data change, feasibility of this newly formed problem cannot be guaranteed a priori. If the resulting problem \mathbb{P}_{t+1} is feasible, the algorithm proceeds with its solution. Otherwise, or if Criterion 1 does not hold, the backup setup described in (46) is used.

Under the backup setup, two situations arise depending on the evolution of the estimates and uncertainty sets.

- (i) *No adaptation of point estimate or uncertainty sets.* If there is no update in the point estimate $\hat{\theta}_t$ and the uncertainty sets Π_t , Ψ_t , and $\tilde{\mathbb{X}}_{0_t}$ after time t , the resulting COCP coincides with a standard robust tube-based MPC formulation. Recursive feasibility then follows directly from the classical robust MPC literature [3], [5], [31], [33].

Let the feasible solution at $t+1$ for this completely non-adaptive scenario (i.e., no update of point estimates or uncertainty sets after t) be denoted using the notation $\underline{(\cdot)}$ as follows:

$$\underline{\mathbb{T}}_{i|t+1}^{\hat{x}} = \alpha_{i+1|t}^* \oplus \beta_{i+1|t}^* \underline{\mathbb{G}}_{t+1} \quad \forall i \in \mathbb{I}_0^{N-1} \quad (51a)$$

$$\underline{\mathbb{T}}_{i|t+1}^u = \{ \mathcal{Z}_2(\underline{\mathfrak{S}}_{i+1|t}^{[j]}, \underline{\mathbb{T}}_{i+1|t}^{\hat{x}}, \underline{\mathbb{T}}_{i+1|t}^u) \mid j \in \mathbb{I}_1^{H_{t+1}} \} \\ \forall i \in \mathbb{I}_0^{N-2} \quad (51b)$$

$$\underline{\mathbb{T}}_{N|t+1}^{\hat{x}} = \alpha_{N|t+1} \oplus \beta_{N|t+1} \underline{\mathbb{G}}_{t+1} \quad (51c)$$

$$\alpha_{N|t+1} = (\hat{A}_t + \hat{B}_t K_t) \alpha_{N|t}^* \quad (51d)$$

$$\beta_{N|t+1} = \min_{\beta} \{ \beta \mid \beta \underline{\mathbb{G}}_{t+1} \supseteq (\hat{A}_t + \hat{B}_t K_t) \beta_{N|t}^* \underline{\mathbb{G}}_t \\ \oplus \underline{\mathcal{E}}_{t+1} \} \quad (51e)$$

$$\underline{\mathbb{T}}_{N-1|t+1}^u = K_t \underline{\mathbb{T}}_{N-1|t+1}^{\hat{x}}. \quad (51f)$$

The feasible solution (51) is adopted as a candidate solution in the next case to establish recursive feasibility.

- (ii) *Adaptation of uncertainty sets with fixed point estimates.* If the point estimates remain unchanged while the uncertainty sets are updated, the following relations hold:

$$\hat{A}_{t+1} = \hat{A}_t, \quad \hat{B}_{t+1} = \hat{B}_t, \quad \hat{x}_{0,t+1} = \hat{x}_{0,t}, \quad (52a)$$

$$\Psi_{t+1} \subseteq \underline{\Psi}_{t+1} = \Psi_t, \quad \Pi_{t+1} \subseteq \underline{\Pi}_{t+1} = \Pi_t, \quad (52b)$$

$$\mathbb{X}_{0,t+1} \subseteq \underline{\mathbb{X}}_{0,t+1} = \mathbb{X}_{0,t}, \quad \tilde{\mathbb{X}}_{0,t+1} \subseteq \underline{\tilde{\mathbb{X}}}_{0,t+1} = \tilde{\mathbb{X}}_{0,t}, \quad (52c)$$

$$\mathcal{D}y_{u_{t+1}} \subseteq \underline{\mathcal{D}y}_{u_{t+1}} = \mathcal{D}y_{u_t}, \quad \mathcal{D}y_{u_{t+1}}^{RPI} \subseteq \underline{\mathcal{D}y}_{u_{t+1}}^{RPI} = \mathcal{D}y_{u_t}^{RPI}, \quad (52d)$$

$$\tilde{\mathbb{X}}_{t+1,i} \subseteq \underline{\tilde{\mathbb{X}}}_{t+1,i} = \tilde{\mathbb{X}}_{t,i+1}, \quad \hat{\mathbb{X}}_{t+1,i} \supseteq \underline{\hat{\mathbb{X}}}_{t+1,i} = \hat{\mathbb{X}}_{t,i+1}, \quad (52e)$$

$$\bar{\mathcal{X}}_{t+1} \subseteq \underline{\bar{\mathcal{X}}}_{t+1} \subseteq \bar{\mathcal{X}}_t, \quad \mathcal{X}_{t+1} \supseteq \underline{\mathcal{X}}_{t+1} \supseteq \mathcal{X}_t, \quad (52f)$$

$$\mathcal{E}_{t+1,i} \subseteq \underline{\mathcal{E}}_{t+1,i} = \mathcal{E}_{t,i+1}, \quad \bar{\mathcal{E}}_{t+1} \subseteq \underline{\bar{\mathcal{E}}}_{t+1} \subseteq \bar{\mathcal{E}}_t, \quad (52g)$$

$$\tilde{\mathbb{X}}_{TS_{t+1}} \supseteq \underline{\tilde{\mathbb{X}}}_{TS_{t+1}} \supseteq \tilde{\mathbb{X}}_{TS_t}, \quad (52h)$$

$$\hat{\mathcal{E}}_{t+1} \subseteq \underline{\hat{\mathcal{E}}}_{t+1} \subseteq \hat{\mathcal{E}}_t, \quad \mathbb{G}_{t+1} \subseteq \underline{\mathbb{G}}_{t+1} \subseteq \mathbb{G}_t. \quad (52i)$$

It is proved that (51), i.e.,

$$\mathbb{T}_{i|t+1}^{\hat{x}} = \underline{\mathbb{T}}_{i|t+1}^{\hat{x}} \quad \forall i \in \mathbb{I}_0^N, \quad \mathbb{T}_{i|t+1}^u = \underline{\mathbb{T}}_{i|t+1}^u \quad \forall i \in \mathbb{I}_0^{N-1} \quad (53a)$$

$$\text{with } \mathbb{G}_{t+1} = \underline{\mathbb{G}}_{t+1} \quad (53b)$$

is also a feasible solution for the COCP at time $t+1$ with adaptation limited to the uncertainty sets.

The tube parameterization satisfies the constraints (41c)-(43), (45b) and (45c) for \mathbb{P}_{t+1} . From (52), it is also observed that

$$\mathbb{T}_{i|t+1}^{\hat{x}} = \underline{\mathbb{T}}_{i|t+1}^{\hat{x}} \subseteq \mathbb{T}_{i+1|t}^{\hat{x}*} \subseteq \hat{\mathbb{X}}_{t,i+1} \subseteq \underline{\hat{\mathbb{X}}}_{t+1,i} \quad \forall i \in \mathbb{I}_0^{N-1}, \quad (54a)$$

$$\mathbb{T}_{N|t+1}^{\hat{x}} = \underline{\mathbb{T}}_{N|t+1}^{\hat{x}} \subseteq \hat{\mathbb{X}}_{TS_{t+1}} \subseteq \underline{\hat{\mathbb{X}}}_{TS_{t+1}}, \quad (54b)$$

$$\mathbb{T}_{i|t+1}^u = \underline{\mathbb{T}}_{i|t+1}^u \subseteq \mathbb{T}_{i+1|t}^u \subseteq \mathbb{U} \quad \forall i \in \mathbb{I}_0^{N-2}, \quad (54c)$$

$$\mathbb{T}_{N-1|t+1}^u = \underline{\mathbb{T}}_{N-1|t+1}^u = K_t \underline{\mathbb{T}}_{N-1|t+1}^{\hat{x}} \subseteq K_t \mathbb{T}_{N|t}^{\hat{x}*} \subseteq \mathbb{U}. \quad (54d)$$

Further, $\forall j \in \mathbb{I}_1^{H_{t+1}}$, the vertices $\mathbf{s}_{i|t+1}^{[j]} \in \mathbb{T}_{i|t+1}^{\hat{x}} = \underline{\mathbb{T}}_{i|t+1}^{\hat{x}}$ and $\mathbf{u}_{i|t+1}^{[j]} \in \mathbb{T}_{i|t+1}^u = \underline{\mathbb{T}}_{i|t+1}^u$ implies

$$\begin{aligned} \hat{A}_t \mathbf{s}_{i|t+1}^{[j]} + \hat{B}_t \mathbf{u}_{i|t+1}^{[j]} &\subseteq \underline{\mathbb{T}}_{i+1|t+1}^{\hat{x}} \ominus \underline{\mathcal{E}}_{t+1,i} \\ &\subseteq \underline{\mathbb{T}}_{i+1|t+1}^{\hat{x}} \ominus \mathcal{E}_{t+1,i} \quad \forall i \in \mathbb{I}_0^{N-1}. \end{aligned} \quad (55)$$

Combining (54) and (55), it is proved that the proposed solution in (51) satisfies all the constraints in \mathbb{P}_{t+1} .

To summarize, it is first shown that the COCP \mathbb{P}_{t+1} might be feasible with a completely new setup; if not, then the backup estimates and sets in (46) leading to the proposed solution (53) ensure that \mathbb{P}_{t+1} is feasible. Therefore, if the COCP (45) with Algorithm 1 is feasible at time t , then it remains feasible at time $t+1$. By repeating the same argument at time $t+1$ under the updated setup, recursive feasibility follows for all subsequent time instants.

APPENDIX V PROOF OF THEOREM 3 PART (2)

Stability is established using the standard MPC Lyapunov argument [1], by considering the optimal cost of the COCP as a candidate Lyapunov function. For the estimated state \hat{x}_t , define

$$J_t(\hat{x}_t, \bar{\mu}_t) \triangleq \sum_{j=1}^{H_t} \Gamma_t^{[j]}, \quad \text{where}$$

$$\Gamma_t^{[j]} \triangleq \sum_{i=0}^{N-1} \left(\|\mathbf{s}_{i|t}^{[j]}\|_Q^2 + \|\mathbf{u}_{i|t}^{[j]}\|_R^2 \right) + \|\mathbf{s}_{N|t}^{[j]}\|_{P_t}^2.$$

From t to $t+1$, the tube geometry and consequently the number of vertices change from H_t to H_{t+1} . This difference is handled using

$$\tilde{\rho}_{1t} \triangleq \begin{cases} 0, & \text{if } H_t \leq H_{t+1} \\ 1, & \text{otherwise,} \end{cases} \quad \tilde{\rho}_{2t} \triangleq \begin{cases} 0, & \text{if } H_t \geq H_{t+1} \\ 1, & \text{otherwise,} \end{cases} \quad (56)$$

$$\text{and } \gamma_1 \triangleq \max_{t \in \mathbb{I}_0^\infty, \hat{x} \in \mathbb{X} \ominus \bar{\mathcal{X}}_0, u \in \mathbb{U}} N \left(\|\hat{x}\|_Q^2 + \|u\|_R^2 \right) + \|\hat{x}\|_{P_{t+1}}^2, \quad (57)$$

which is finite by Lemma 1, Theorems 1, 2, and 3 Part (1).

From Appendix IV, the quantities $\mathbf{s}_{i|t+1}^{[j]}$ and $\mathbf{u}_{i|t+1}^{[j]}, \forall j \in \mathbb{I}_1^{H_{t+1}}$, represent the vertices of $\underline{\mathbb{T}}_{i|t+1}^{\hat{x}}$ and the corresponding elements of $\underline{\mathbb{T}}_{i|t+1}^u$ defined in (51), respectively. The worst-case scenario is considered with $\mathbb{G}_{t+1} = \underline{\mathbb{G}}_{t+1}$ and $H_{t+1} = H_{t+1}$. At any time $t+1$, where $t \in \mathbb{I}_0^\infty$, it follows that

$$\begin{aligned} J_{t+1}^*(\hat{x}_{t+1}) &\leq J_{t+1}(\hat{x}_{t+1}, \mu_{t+1}) = \sum_{j=1}^{H_{t+1}} \Gamma_{t+1}^{[j]} \\ &= \sum_{j=1}^{H_t} \Gamma_{t+1}^{[j]} - \tilde{\rho}_{1t} \sum_{j=H_{t+1}+1}^{H_t} \Gamma_{t+1}^{[j]} + \tilde{\rho}_{2t} \sum_{j=H_t+1}^{H_{t+1}} \Gamma_{t+1}^{[j]} \\ &\leq \sum_{j=1}^{H_t} \left(\sum_{i=0}^{N-1} \left(\|\mathbf{s}_{i|t+1}^{[j]}\|_Q^2 + \|\mathbf{u}_{i|t+1}^{[j]}\|_R^2 \right) + \|\mathbf{s}_{N|t+1}^{[j]}\|_{P_{t+1}}^2 \right) \\ &\quad + \tilde{\rho}_{2t} (H_{t+1} - H_t) \gamma_1 \quad (\text{using (57)}) \\ &= \sum_{j=1}^{H_t} \left(\sum_{i=0}^{N-1} \left(\|\mathbf{s}_{i|t+1}^{[j]}\|_Q^2 + \|\mathbf{u}_{i|t+1}^{[j]}\|_R^2 \right) + \|\mathbf{s}_{N|t+1}^{[j]}\|_{P_{t+1}}^2 \right) \\ &\quad + \tilde{\rho}_{2t} (H_{t+1} - H_t) \gamma_1 \quad (\text{using (54)}) \\ &\leq \sum_{j=1}^{H_t} \left(\sum_{i=0}^{N-2} \left(\|\mathbf{s}_{i+1|t}^{[j]*}\|_Q^2 + \|\mathbf{u}_{i+1|t}^{[j]*}\|_R^2 \right) + \|\mathbf{s}_{N|t+1}^{[j]}\|_{P_{t+1}}^2 \right. \\ &\quad \left. + \|\mathbf{s}_{N|t}^{[j]*}\|_{Q+K_t^\top R K_t}^2 \right) + \tilde{\rho}_{2t} (H_{t+1} - H_t) \gamma_1 \quad (\text{using (54)}) \end{aligned}$$

$$\begin{aligned}
 &= J_t^*(\hat{x}_t) - \sum_{j=1}^{H_t} \left(\left\| \mathfrak{s}_{0|t}^{[j]*} \right\|_Q^2 + \left\| \mathfrak{u}_{0|t}^{[j]*} \right\|_R^2 + \left\| \mathfrak{s}_{N|t}^{[j]*} \right\|_{P_t}^2 \right) \\
 &+ \sum_{j=1}^{H_t} \left(\left\| (\hat{A}_{t+1} + \hat{B}_{t+1}K_{t+1})\mathfrak{s}_{N|t}^{[j]*} + \varepsilon_{t+1, N-1} \right\|_{P_{t+1}}^2 \right. \\
 &\quad \left. + \left\| \mathfrak{s}_{N|t}^{[j]*} \right\|_{Q+K_t^\top RK_t}^2 \right) + \tilde{\rho}_{2_t}(H_{t+1} - H_t)\gamma_1 \\
 &\leq (1 - \gamma_2)J_t^*(\hat{x}_t) + \tilde{\rho}_{2_t}(H_{t+1} - H_t)\gamma_1 \\
 &+ \sum_{j=1}^{H_t} \left(- \left\| \mathfrak{s}_{N|t}^{[j]*} \right\|_{P_t}^2 + \left\| \mathfrak{s}_{N|t}^{[j]*} \right\|_{Q+K_t^\top RK_t}^2 \right. \\
 &\quad \left. + \left\| \mathfrak{s}_{N|t}^{[j]*} \right\|_{(\hat{A}_{t+1} + \hat{B}_{t+1}K_{t+1})^\top P_{t+1}(\hat{A}_{t+1} + \hat{B}_{t+1}K_{t+1})}^2 \right) \\
 &+ H_t \max_{t \in \mathbb{I}_0^\infty, \varepsilon \in \tilde{\mathcal{E}}_t} \|\varepsilon\|_{P_{t+1}}^2, \text{ (by Cauchy-Schwartz inequality)}
 \end{aligned}$$

where $\gamma_2 \triangleq \frac{\sum_{j=1}^{H_t} (\left\| \mathfrak{s}_{0|t}^{[j]*} \right\|_Q^2 + \left\| \mathfrak{u}_{0|t}^{[j]*} \right\|_R^2)}{J_t^*(\hat{x}_t)} \Rightarrow \gamma_2 \in (0, 1] \Rightarrow 1 - \gamma_2 \in [0, 1)$ (by definition of J_t^*).

Irrespective of whether new point estimates satisfying Criterion 1 are used, or the setup in (46) is employed, the following holds:

$$\begin{aligned}
 P_t - (\hat{A}_{t+1} + \hat{B}_{t+1}K_{t+1})^\top P_{t+1}(\hat{A}_{t+1} + \hat{B}_{t+1}K_{t+1}) \\
 - Q - K_t^\top RK_t \succeq 0,
 \end{aligned}$$

which implies

$$\begin{aligned}
 J_{t+1}^*(\hat{x}_{t+1}) \leq (1 - \gamma_2)J_t^*(\hat{x}_t) + \tilde{\rho}_{2_t}(H_{t+1} - H_t)\gamma_1 \\
 + H_t \max_{t \in \mathbb{I}_0^\infty, \varepsilon \in \tilde{\mathcal{E}}_t} \|\varepsilon\|_{P_{t+1}}^2.
 \end{aligned}$$

For implementation, an upper bound H_{\max} is imposed on the number of vertices of \mathbb{G}_t . Due to recursive feasibility and bounded sets \mathbb{D} , Ψ_0 and \mathbb{X}_{0_0} , $\max_{t \in \mathbb{I}_0^\infty, \varepsilon \in \tilde{\mathcal{E}}_t} \|\varepsilon\|_{P_{t+1}}^2$ is bounded. The matrices P_{t+1} are also bounded since they appear in the cost function. Therefore, defining

$$\gamma_3 \triangleq H_{\max} \max_{t \in \mathbb{I}_0^\infty, \varepsilon \in \tilde{\mathcal{E}}_t} \|\varepsilon\|_{P_{t+1}}^2 + (H_{\max} - H_{\min})\gamma_1,$$

yields

$$J_{t+1}^*(\hat{x}_{t+1}) \leq (1 - \gamma_2)J_t^*(\hat{x}_t) + \gamma_3.$$

This implies that \exists constants $c_1 > 0$, $c_2 \in (0, 1)$ and $c_3 > 0$ such that

$$\|\hat{x}_t\| \leq c_1 c_2^t \|\hat{x}_0\| + c_3 \quad \forall t \in \mathbb{I}_0^\infty,$$

thereby establishing robust exponential stability of the adaptive observer.

Further, once learning has converged, H_t remains constant and the term $H_{t+1} - H_t$ becomes zero. Consequently, the observer state converges to a bounded set determined by \mathbb{D} , Ψ_t , \mathbb{X}_{0_t} , and the bounded quantities P_t , K_t , \hat{A}_t , \hat{B}_t , and \hat{x}_{0_t} .

Since the estimation error is bounded by $\tilde{\mathbb{X}}_{0_t}$, which is non-increasing, robust exponential stability of the actual plant (1) also follows.

APPENDIX VI PROOF OF THEOREM 4

With no change in the point estimates and the uncertainty sets, the observer state can be expressed as

$$\begin{aligned}
 \hat{x}_{t+1} &= M_{t+1}\hat{p} + F^{t+1}\hat{x}_0 = (FM_t + [Y_t \ U_t])\hat{p} + F^{t+1}\hat{x}_0 \\
 &= F\hat{x}_t + (\hat{A}_t - F)x_t + \hat{B}_t u_t,
 \end{aligned}$$

where the time indices are not used in \hat{p} and \hat{x}_0 to represent they are unchanged. Subtracting from (1a) yields

$$\tilde{x}_{t+1} = F\tilde{x}_t + (A - \hat{A}_t)x_t + (B - \hat{B}_t)u_t + d_t. \quad (58)$$

Now, consider the case of a Luenberger observer-based output feedback MPC [31]–[33], where nominal parameters \hat{A} , \hat{B} are selected to generate a nominal and error dynamics, and a gain L_{obs} is chosen such that $\hat{A} - L_{obs}C$ is Schur stable. The system state and observer state are expressed as

$$z_{t+1} = \hat{A}z_t + \hat{B}u_t + \underbrace{(A - \hat{A})z_t + (B - \hat{B})u_t + d_t}_{\text{lumped additive disturbance}},$$

$$\hat{z}_{t+1} = \hat{A}\hat{z}_t + \hat{B}u_t + L_{obs}(Cz_t - C\hat{z}_t),$$

respectively. The observer state estimation error dynamics becomes

$$\tilde{z}_{t+1} = (\hat{A} - L_{obs}C)\tilde{z}_t + (A - \hat{A})z_t + (B - \hat{B})u_t + d_t,$$

which is similar to (58) since both F and $(\hat{A} - L_{obs}C)$ are Schur stable; the dynamics becomes equal provided F is chosen to be equal to $(\hat{A} - L_{obs}C)$. This also highlights the certainty equivalence principle used in designing adaptive observers. The remaining proof follows from the existing literature [3], [31], [33].

REFERENCES

- [1] B. Kouvaritakis and M. Cannon, “Model Predictive Control,” *Cham, Switzerland: Springer International*, vol. 38, 2016.
- [2] J. B. Rawlings, D. Q. Mayne, and M. M. Diehl, *Model Predictive Control: Theory, Computation, and Design*. Nob Hill Publishing, LLC, 2017.
- [3] L. Chisci, J. Rossiter, and G. Zappa, “Systems with persistent disturbances: predictive control with restricted constraints,” *Automatica*, vol. 37, no. 7, pp. 1019–1028, 2001.
- [4] W. Langson, I. Chrysoschoos, S. Raković, and D. Q. Mayne, “Robust model predictive control using tubes,” *Automatica*, vol. 40, no. 1, pp. 125–133, 2004.
- [5] S. V. Raković, B. Kouvaritakis, R. Findeisen, and M. Cannon, “Homothetic tube model predictive control,” *Automatica*, vol. 48, no. 8, pp. 1631–1638, 2012.
- [6] J. Fleming, B. Kouvaritakis, and M. Cannon, “Robust tube MPC for linear systems with multiplicative uncertainty,” *IEEE Transactions on Automatic Control*, vol. 60, no. 4, pp. 1087–1092, 2015.
- [7] M. V. Kothare, V. Balakrishnan, and M. Morari, “Robust constrained model predictive control using linear matrix inequalities,” *Automatica*, vol. 32, no. 10, pp. 1361–1379, 1996.
- [8] M. Bujarbaruah, U. Rosolia, Y. R. Stürz, and F. Borrelli, “A simple robust MPC for linear systems with parametric and additive uncertainty,” in *American Control Conference*, 2021, pp. 2108–2113.
- [9] S. Jafari Fesharaki, M. Kamali, and F. Sheikholeslam, “Adaptive tube-based model predictive control for linear systems with parametric uncertainty,” *IET Control Theory & Applications*, vol. 11, no. 17, pp. 2947–2953, 2017.
- [10] A. Dhar and S. Bhasin, “Indirect adaptive MPC for discrete-time LTI systems with parametric uncertainties,” *IEEE Transactions on Automatic Control*, vol. 66, no. 11, pp. 5498–5505, 2021.

- [11] J. Köhler, E. Andina, R. Soloperto, M. A. Müller, and F. Allgöwer, "Linear robust adaptive model predictive control: Computational complexity and conservatism," in *IEEE Conference on Decision and Control*, 2019, pp. 1383–1388.
- [12] M. Lorenzen, M. Cannon, and F. Allgöwer, "Robust MPC with recursive model update," *Automatica*, vol. 103, pp. 461–471, 2019.
- [13] X. Lu and M. Cannon, "Robust adaptive model predictive control with persistent excitation conditions," *Automatica*, vol. 152, p. 110959, 2023.
- [14] A. Dey and S. Bhasin, "Adaptive output feedback MPC with guaranteed stability and robustness," *IEEE Transactions on Automatic Control*, vol. 70, no. 12, pp. 8345–8352, 2025.
- [15] A. Dey, A. Dhar, and S. Bhasin, "Adaptive output feedback model predictive control," *IEEE Control Systems Letters*, vol. 7, pp. 1129–1134, 2023.
- [16] X. Lu and M. Cannon, "Robust adaptive tube model predictive control," in *American Control Conference*, 2019, pp. 3695–3701.
- [17] M. Kögel and R. Findeisen, "Robust MPC with reduced conservatism blending multiples tubes," in *American Control Conference*, 2020, pp. 1949–1954.
- [18] D. Tranos, A. Russo, and A. Proutiere, "Self-tuning tube-based model predictive control," in *American Control Conference*, 2023, pp. 3626–3632.
- [19] K. Wang, S. Zhang, S. Gros, and S. V. Raković, "Tube MPC with time-varying cross-sections," *IEEE Transactions on Automatic Control*, vol. 70, no. 3, pp. 1851–1858, 2025.
- [20] P. P. Khargonekar, I. R. Petersen, and K. Zhou, "Robust stabilization of uncertain linear systems: quadratic stabilizability and H^∞ control theory," *IEEE Transactions on Automatic Control*, vol. 35, no. 3, pp. 356–361, 1990.
- [21] P. Gahinet and P. Apkarian, "A linear matrix inequality approach to H^∞ control," *International Journal of Robust and Nonlinear Control*, vol. 4, no. 4, pp. 421–448, 1994.
- [22] B. R. Barmish, "Necessary and sufficient conditions for quadratic stabilizability of an uncertain system," *Journal of Optimization Theory and Applications*, vol. 46, no. 4, pp. 399–408, 1985.
- [23] I. Petersen, "Quadratic stabilizability of uncertain linear systems: Existence of a nonlinear stabilizing control does not imply existence of a linear stabilizing control," *IEEE Transactions on Automatic Control*, vol. 30, no. 3, pp. 291–293, 1985.
- [24] J. Berberich, J. Köhler, M. A. Müller, and F. Allgöwer, "Data-driven model predictive control with stability and robustness guarantees," *IEEE Transactions on Automatic Control*, vol. 66, no. 4, pp. 1702–1717, 2020.
- [25] J. Coulson, J. Lygeros, and F. Dörfler, "Data-enabled predictive control: In the shallows of the DeePC," in *European Control Conference*, 2019, pp. 307–312.
- [26] R. Kosut, M. Lau, and S. Boyd, "Set-membership identification of systems with parametric and nonparametric uncertainty," *IEEE Transactions on Automatic Control*, vol. 37, no. 7, pp. 929–941, 1992.
- [27] G. Kreisselmeier, "Adaptive observers with exponential rate of convergence," *IEEE Transactions on Automatic Control*, vol. 22, no. 1, pp. 2–8, 1977.
- [28] P. M. Lion, "Rapid identification of linear and nonlinear systems," *AIAA Journal*, vol. 5, no. 10, pp. 1835–1842, 1967.
- [29] A. Dey, S. Bandyopadhyay, and S. Bhasin, "Initial excitation-based adaptive observers for discrete-time LTI systems," in *European Control Conference*, 2026, to appear. [Online]. Available: <https://arxiv.org/abs/2511.13117>
- [30] L. Chisci, A. Garulli, A. Vicino, and G. Zappa, "Block recursive parallelotopic bounding in set membership identification," *Automatica*, vol. 34, no. 1, pp. 15–22, 1998.
- [31] M. Kögel and R. Findeisen, "Robust output feedback MPC for uncertain linear systems with reduced conservatism," *IFAC-PapersOnLine*, vol. 50, no. 1, pp. 10685–10690, 2017.
- [32] D. Q. Mayne, S. V. Raković, R. Findeisen, and F. Allgöwer, "Robust output feedback model predictive control of constrained linear systems," *Automatica*, vol. 42, no. 7, pp. 1217–1222, 2006.
- [33] D. Q. Mayne, S. Raković, R. Findeisen, and F. Allgöwer, "Robust output feedback model predictive control of constrained linear systems: Time varying case," *Automatica*, vol. 45, no. 9, pp. 2082–2087, 2009.
- [34] S. V. Rakovic, E. C. Kerrigan, K. I. Kouramas, and D. Q. Mayne, "Invariant approximations of the minimal robust positively invariant set," *IEEE Transactions on Automatic Control*, vol. 50, no. 3, pp. 406–410, 2005.
- [35] P. Ioannou and B. Fidan, *Adaptive Control Tutorial*. SIAM, 2006.
- [36] A. Dey and S. Bhasin, "Computation of maximal admissible robust positive invariant sets for linear systems with parametric and additive uncertainties," *IEEE Control Systems Letters*, vol. 8, pp. 1775–1780, 2024.
- [37] H. M. S. M. Veres and J. of P. Norton, "Limited-complexity model-unfalsifying adaptive tracking-control," *International Journal of Control*, vol. 72, no. 15, pp. 1417–1426, 1999.
- [38] G. Marafioti, R. R. Bitmead, and M. Hovd, "Persistently exciting model predictive control," *International Journal of Adaptive Control and Signal Processing*, vol. 28, no. 6, pp. 536–552, 2014.